Quaternary sector collapses of Nevado de Toluca volcano (Mexico) governed by regional tectonics and volcanic evolution

G. Norini
L. Capra
Centro de Geociencias, Universidad Nacional Autónoma de México, Campus Juriquilla-UNAM, Querétaro, Qro. 76230, Mexico

G. Groppelli
Istituto per la Dinamica dei Processi Ambientali, Sezione di Milano, Consiglio Nazionale delle Ricerche, Via Mangiagalli 34, 20133 Milano, Italy

A.M.F. Lagmay
National Institute of Geological Science, Velasquez St. corner Garcia St., University of the Philippines, 1101 Quezon City, Philippines

ABSTRACT

Nevado de Toluca volcano is an andesitic-dacitic composite volcano of Late Pliocene–Holocene age located in the central-eastern sector of the Trans-Mexican Volcanic Belt, an active continental arc. The latest stage of Nevado de Toluca evolution, in the past 50 k.y., has shown an interplay between volcanic activity and kinematics of the basement structures. Geological mapping, stratigraphic analysis, morphological and structural interpretation, and analogue modeling were used to investigate these complex volcano-tectonics relationships. In the past 50 k.y., Nevado de Toluca volcano underwent at least three sector collapses on the east, east-southeast, and west flanks because of faulting and destabilization of young dacitic domes at its summit. Field and remotely sensed data supported by analogue models of transtensive basement tectonics revealed that these catastrophic events were strongly correlated to the presence of the east-west–striking active Tenango fault system. The geometry, kinematics, and dynamics of the basement structure controlled the growth of a dome complex in the volcano summit and its destabilization. As a consequence of the active basement tectonics, the most probable sector collapse directions in the case of future gravitational failures of the volcano summit will be east-southeast, west-northwest, east, and west. Nevado de Toluca poses potential hazards to more than 25 million inhabitants; the analysis presented in this paper can improve hazard mitigation on the basis of better knowledge of growth and collapse mechanism of the volcano. The numerous examples of composite volcanoes in continental and island volcanic arcs with similar structural-volcanological characteristics of Nevado de Toluca volcano imply that the model results can also act as a guide to study the growth and collapse of other composite volcanoes affected by basement structures.

INTRODUCTION

Composite volcanoes are highly dynamic structures characterized by alternating periods of growth and quiescence, both marked by episodes of instability that can lead to slope failures ranging from moderate and localized to voluminous, involving a significant portion of the edifice. The instability can develop over thousands of years, or over only a few days. A slowly developing instability may be accelerated by a discrete event and culminate in catastrophic failure. In many cases, destabilization is produced by a combination of circumstances and events, rather than a single cause (Voight and Elsworth, 1997). A volcano can be rendered unstable by flank overloading from deposition of volcanic products (Murray, 1988), dike intrusion (Siebert, 1984; Elsworth and Voight, 1996), cryptodome growth beneath and inside the volcano (Lipman and Mullineaux, 1981; Donnadieu and Merle, 1998), hydrothermal alteration (Day, 1996; Voight and Elsworth, 1997; Finn et al., 2004), steepening of slopes (Siebert, 1984), gravitational spreading (Borgia et al., 2000) and tectonic activity of the basement (Moriya, 1980; Siebert, 1984; Ui et al., 1986; Tibaldi, 1995; Lagmay et al., 2000; Vidal and Merle, 2000; Norini and Lagmay, 2005). Stress-field orientation has been recognized as an important factor governing the directions of collapse in composite volcanoes since 1977, when Nakamura showed that cone elongation, fractures, strike of dikes, and alignments of flank vents occur parallel to the regional maximum horizontal stress. Moriya (1980) applied Nakamura's (1977) model to 30 volcano amphitheater craters in Japan, and concluded that dike intrusions promote lateral collapses perpendicular to the maximum horizontal stress direction. Siebert (1984) noted from the global database of volcano sector collapses that dike swarms parallel to the maximum horizontal stress induce instability, often promoting collapses normal to the dominant direction of dike emplacement. Not all volcanoes, however, share the same relationship between regional stress and instability. In a study of 52 Japanese Quaternary volcanoes with associated debris avalanche deposits, Ui et al. (1986) found no relation between the direction of amphitheater craters and the maximum horizontal stress. Bahar and Girod (1983) showed that in Indonesian volcanoes the direction of dikes and the alignments of vents and volcanic cones tend to form at an angle relative to the direction of maximum horizontal stress, and are related to regional structures. These observations suggest that the relationship between regional stress and volcano instability is more complex than previously thought, and that other factors may govern the direction of sector collapses. One such factor may be the role of tectonic structures in the basements underlying

Geosphere; October 2008; v. 4; no. 5; p. 854–871; doi: 10.1130/GES00165.1; 16 figures; 1 table; 1 animation; 1 supplemental file.

volcanoes. Francis and Wells (1988) examined the influence of structural setting and tectonic activity in generating volcano instability in 28 examples of breached cones in the Andes. In most cases, breaching occurred perpendicular to the main lineaments and fractures. In contrast, cone breaching and lateral collapse parallel to the fault strike are more common in regions of transcurrent and transtensive faulting (Tibaldi, 1995). Van Wyk de Vries and Merle (1998) and Lagmay et al. (2000) studied the effects of transcurrent faulting on the stability of volcanoes by performing analogue model experiments that demonstrated that edifice instability can be generated by an underlying active strike-slip fault. The instability and consequent landslides were oriented ~10°–30° from the trend of the main strike-slip fault (Lagmay et al., 2000; Wooller, 2004; Norini and Lagmay, 2005; Lagmay and Valdivia, 2006).

NEVADO DE TOLUCA VOLCANO

The Late Pliocene–Holocene age Nevado de Toluca volcano, one of the most prominent volcanic features within the Trans-Mexican Volcanic Belt, is the fourth highest peak in Mexico; it has an altitude of 4680 m above sea level, and is located 80 km west-southwest of Mexico City and 23 km southwest of the city of Toluca (Fig. 1). Its past activity has affected an area now inhabited by more than 25 million people; thus, the hazards it poses are of serious concern. The latest phase of volcanism started ca. 50 ka and consists of dacitic domes mantled by pyroclastic and epiclastic deposits (García-Palomo et al., 2002; Bellotti et al., 2006). During the past 50 k.y., five major plinian eruptions and at least five dome collapses with major events of block and ash flows at 37 and 28 ka yielded a thick sequence of pyroclastic deposits surrounding the volcano (Bloomfield and Valastro, 1974, 1977; Macías et al., 1997; García-Palomo et al., 2002; Arce et al., 2003, 2005; Capra et al., 2006). The volcano is located at the intersection of three fault systems, the Taxco-Querétaro, the San Antonio, and the still active Tenango (García-Palomo et al., 2000; Bellotti et al., 2006; Norini et al., 2006) (Fig. 1B).

MOTIVATION AND OBJECTIVES

This study was prompted by the recent availability of a complete stratigraphic and structural record of Nevado de Toluca volcano (Bellotti et al., 2004, 2006; Norini et al., 2004, 2006). Numerous composite volcanoes like Pico de Orizaba, Popocatépetl, Nevado de Toluca, and the Colima Volcanic Complex are built along the Trans-Mexican Volcanic Belt, an active continental volcanic arc (Ferrari, 2000) (Fig. 1A). Each of these volcanoes has undergone sector failures in the past, and it may undergo debris avalanches and lahars again (Capra et al., 2002). Thus, better understanding of these catastrophic events with respect to time of recurrence during the lifespan of a volcano and their relation to underlying basement structures is necessary.

Previously, the relationships between volcano edifice collapse and tectonics were mainly based on statistical studies of several natural cases and on analogue modeling (Moriya, 1980; Siebert, 1984; Ui et al., 1986; Francis and Wells, 1988; Tibaldi, 1995). Here we propose a model based on the spatial and temporal interaction of volcanic processes and fault mechanics within a single well-known natural example, the Nevado de Toluca volcano. Our approach is to complement geometric relationships between fault lines and direction of collapse and detailed stratigraphic and structural data collected in the field with analogue modeling in order to develop a model for the growth and collapse of the volcano that matches the present volcano structure as well as mechanism of collapse during the past 50 k.y.

FIELD METHODS

How Nevado de Toluca volcano evolved over the past 50 k.y. and how the structural history of the basement affected the stability of its edifice were determined from extensive field mapping at a scale of 1:25,000, reduced to 1:50,000 in the new geological map (Bellotti et al., 2004). All these data were used as input for a geographic information system (GIS) from which the maps presented in this paper were extracted (Supplemental File 1[1]). The past 50 k.y. of Nevado de Toluca evolution is the most important period for hazard evaluation and the main focus of this paper. We studied lithostratigraphic units belonging to this phase in detail, with emphasis on the structures of the summit dacitic domes and stratigraphic relationships of debris avalanche deposits. A paleosol layer at the base of a debris avalanche deposit on the eastern flank of the volcano (Arroyo Grande deposit) was ^{14}C dated. The volumes of the debris avalanche deposits were estimated by means of interpolation in a GIS using deposit thickness measurements. Linear interpolation of the deposit thickness among outcrops resulted in a raster file representing the spatial variation of thickness, from which the total volume was obtained.

Structural analyses of Nevado de Toluca volcano and surrounding areas were performed by García-Palomo et al. (2000), Bellotti et al. (2006), and Norini et al. (2006). Previously published descriptive analysis and kinematic interpretation of morphostructural lineaments and structural stations revealed the age and kinematics of the complex set of faults that cross the volcanic edifice and its basement (García-Palomo et al., 2000; Bellotti et al., 2006; Norini et al., 2006). We performed supplementary morphostructural and geological analyses at the volcano and crater scales to account for the effect of the active Tenango fault system on Nevado de Toluca volcano. At the volcano scale, analysis of a digital elevation model obtained by interpolation of the 1:50,000 Instituto Nacional de Estadística Geografía y Informática (INEGI) contour lines with an interval of 20 m was used to delineate the major structures affecting the volcano edifice. At the same scale, a GIS was used as the basis for spatial analysis of the lithostratigraphic units. The GIS database incorporated all the geological data representing the growth of the volcano and led to visualize the feeding system geometry. At the crater scale, morphostructural analysis of the summit dacitic domes was performed to constrain the orientations of measured structural lineaments, which were probably derived from the most recent phase of basement tectonics. Dome feeding systems are not visible in the field, and erosion and tectonic dissection have obscured eruptive fissures. We used the directions of dome elongation as proxy to identify the local tectonic grain. In fact, even if the morphology of domes is also controlled by topography and explosive volcanic activity that shaped the crater area, the elongation of these monogenic edifices mainly reflects the feeding-system orientation and the direction of the tectonic structures that controlled dome growth and faulting (Nakamura, 1977; Fink and Pollard, 1983; Anderson and Fink, 1990; Pasquaré and Tibaldi, 2003; Schilling et al., 2006). Therefore, the azimuths of summit dome elongations were measured in aerial photographs with GIS software and plotted in rose diagrams to support our structural interpretation.

[1]Supplemental File 1. Geographic information system (GIS) database. Geological map of the domes and debris avalanche deposits younger than 50 ka, main structures of the Tenango fault system traversing the Nevado de Toluca edifice, and topography (contour lines every 100 m, Instituto Nacional de Estadística Geografía y Informática [INEGI]). The database files are in shapefile format (ESRI) and are compatible with free and open source software (e.g., Quantum GIS, http://download.qgis.org/downloads.rhtml). If you are viewing the PDF of this paper or reading it offline, please visit http://dx.doi.org/10.1130/GES00165.S1 (Supplemental File 1) or the full-text article on www.gsajournals.org to view Supplemental File 1.

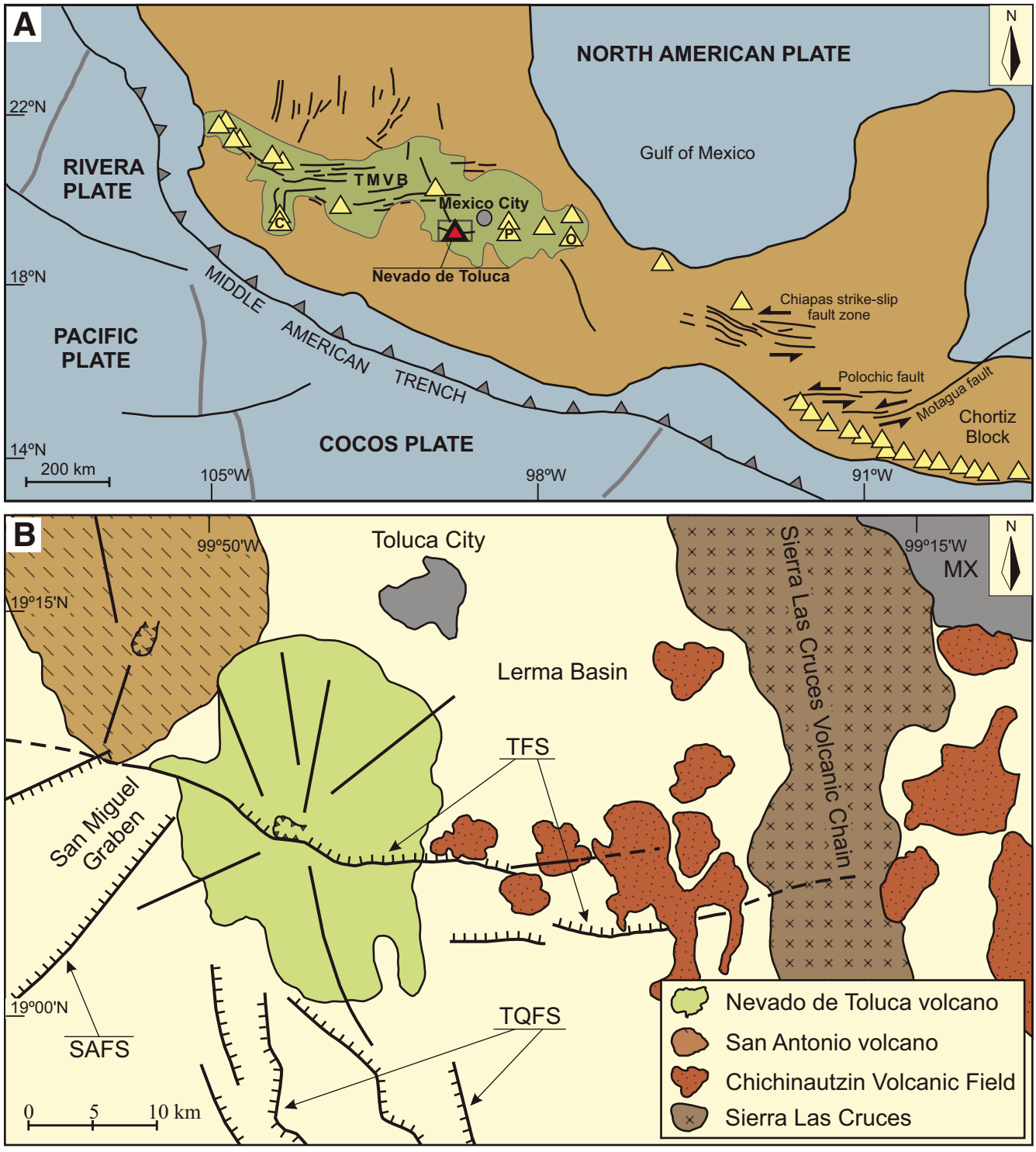

Figure 1. (A) Location of the Trans-Mexican Volcanic Belt (TMVB) in the geodynamic framework of North and Central America. Triangles show major volcanoes. O—Pico de Orizaba; P—Popocatépetl; C—Colima Volcanic Complex. Solid black lines are major faults. (B) Outline map with the location of the Tenango, San Antonio, and Taxco-Querétaro fault systems and the main volcanoes in the Nevado de Toluca area. MX—Mexico City; TQFS—Taxco-Querétaro fault system; SAFS—San Antonio fault system; TFS—Tenango fault system (locations of fault systems are from García-Palomo et al., 2000).

DATA COLLECTION AND ANALYSES

Geological Data

The geological data collected during this work, integrated with those in the literature (Cantagrel et al., 1981; Macías et al., 1997; García-Palomo et al., 2002; Bellotti et al., 2004; Norini et al., 2004), reveal that Nevado de Toluca volcano mainly consists of a stratocone with an age of 2.6–1 Ma (Fig. 2). After a period of quiescence, a small dome complex formed atop the stratovolcano beginning 50 ka, periodically interrupted by explosive activity. The last major plinian eruption of the volcano, dated as 10.5 ka (Bloomfield and Valastro, 1974; Bloomfield and Valastro, 1977; Macías et al., 1997; Arce et al., 2003), produced a fall deposit, the Upper Toluca Pumice, which covers nearly the entire Nevado de Toluca edifice and vicinity. This deposit is drawn separately as Figure 2A because it hides the underlying geology, which is revealed in Figure 2B. A cross section (Fig. 2C) derived from the geology and the Tenango fault system geometry (Norini et al., 2006) shows the summit dome complex above the older stratocone, whose flanks are partly covered by more recent volcaniclastic deposits. The dome complex consists of 14 individual domes that are stratigraphically well constrained because they are above the unconformity that bounds the top of the old stratovolcano (Fig. 3; Supplemental File 1 [see footnote 1]). Stratigraphic relationships between individual domes are not always clear because their contacts are usually masked by thick talus deposits. Tephrochronology suggests an age of 42 ka as the most probable start of the volcanic activity in the crater area, represented by the Pink Pumice Flow deposit (Macías et al., 1997). A ^{14}C age of 37 ka for the dome complex was obtained indirectly from a block and ash flow deposit that is geochemically related to the El Fraile dome

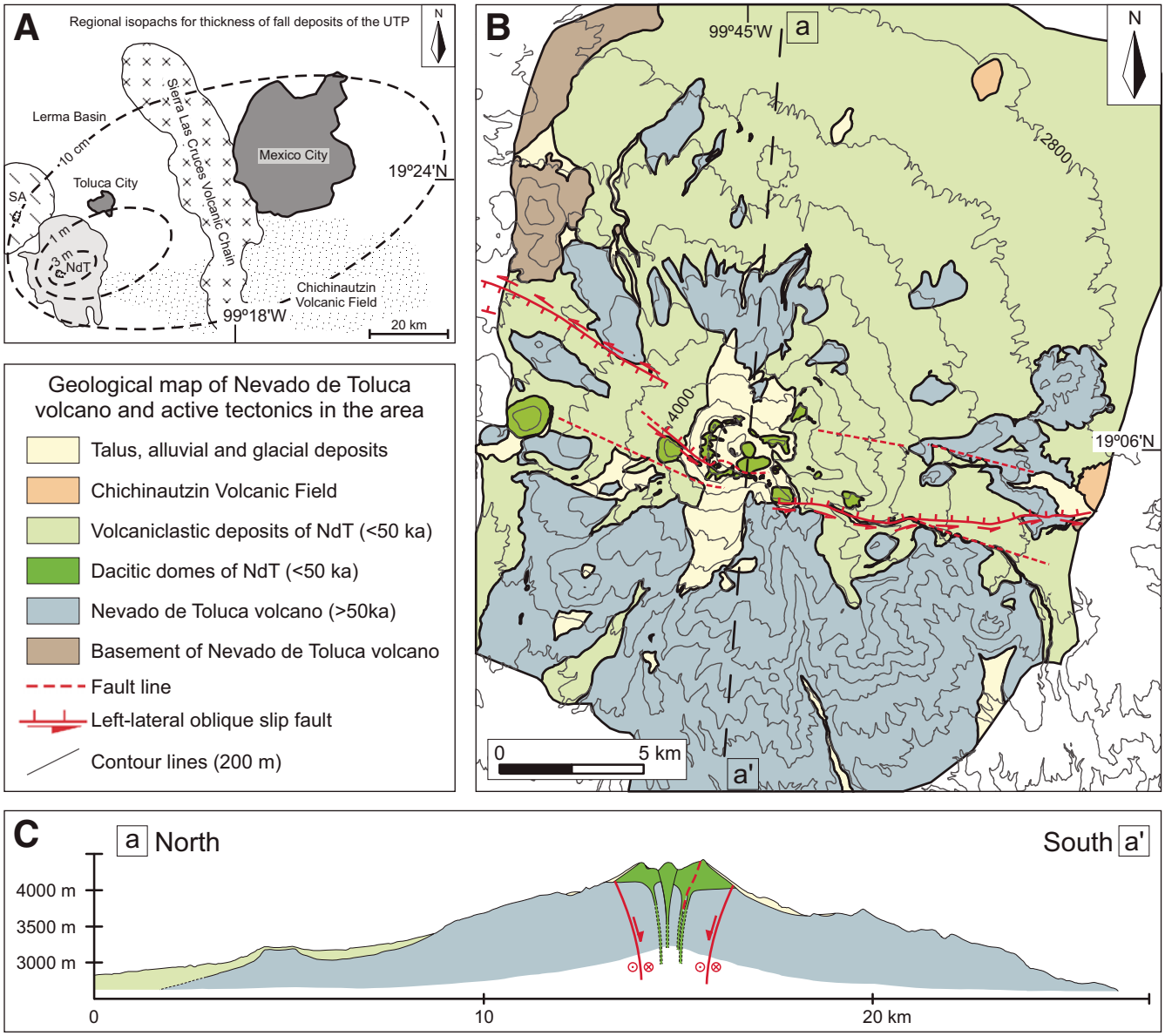

Figure 2. (A) Regional isopachs for thickness of fall deposit of the Upper Toluca Pumice (UTP) (modified from Arce et al., 2003). SA—San Antonio Volcano. (B) Schematic geological map of the Nevado de Toluca (NdT) Volcano. (C) Schematic geological cross section of Nevado de Toluca Volcano.

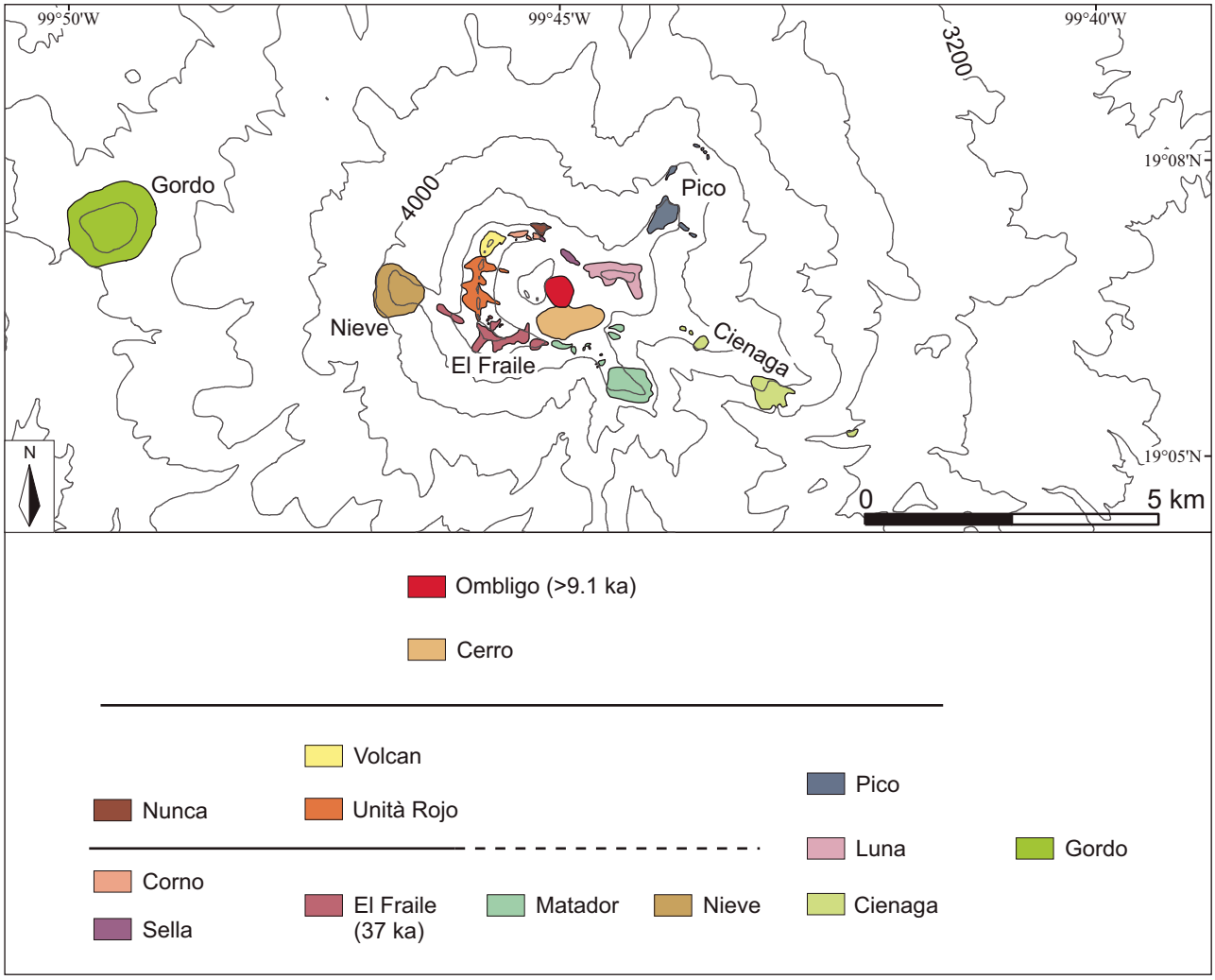

Figure 3. Geological map of the dacitic dome complex (contour every 200 m) and stratigraphic relationships among domes.

(Macías et al., 1997; M. D'Antonio, 2005, personal commun.). The El Ombligo dome exposed in the summit crater of the volcano is the youngest element of the dome complex and has a minimum age of 9100 ± 500 yr (Arce et al., 2003). To summarize, the activity of the summit dome complex was mainly concentrated between ca. 42 ka and 9 ka.

The geological map compiled during this work allows an accurate analysis of the spatial and temporal distribution of the lithostratigraphic units (Fig. 3; Supplemental File 1 [see footnote 1]). It shows that the dome complex (younger than 50 ka) is mainly confined to the crater area, although some domes, including the Gordo, are rather far from the summit (Figs. 2B and 3). The evolution of the crater area can be divided into three stages based on the stratigraphic and geometric relationships among summit domes (Fig. 3). In the first stage the domes, including the El Fraile dome, that compose the southern and northern crater rims were emplaced, whereas in the second stage at least two major domes were emplaced along the present western wall of the crater rim (Fig. 3). During the third stage of evolution, at least two domes, including the El Ombligo, formed in the central portion of the crater, representing the youngest effusive products of volcano (Fig. 3). An estimate of the actual volume of the dome complex was performed considering its base at 3900–4000 m above sea level (Fig. 2C). The volume estimate of 5–6 km^3 was obtained by subtracting the actual topography from the dome complex base in a GIS. Among the volcaniclastic deposits emplaced on the volcano flanks in the past 50 k.y., those that are directly related to sector and flank collapses are the debris avalanche deposits. The only previously described debris avalanche deposit younger than 50 ka was deposited on Nevado de Toluca's eastern flank (Macías et al., 1997; Arce et al., 2003). Our field work identified three debris avalanche deposits on the volcano for which stratigraphic analysis and ^{14}C dating revealed a young age indicating that they are related to gravitational instability of Nevado de Toluca during the past 50 k.y. These catastrophic events emplaced volcaniclastic deposits in deep gullies such as the Arroyo Grande and El Zaguán, which funneled the debris 5–9 km away from the source. We have named the three debris avalanche deposits the Arroyo Grande, El Zaguán, and Nopal lithostratigraphic units, which are respectively distributed to the east-southeast, east, and west-northwest of the summit (Fig. 4; Supplemental File 1 [see footnote 1]).

The Arroyo Grande unit crops out along the Arroyo Grande ravine and has a maximum thickness of ~60 m and an estimated volume of 0.35 km^3. Hummocky morphology is still recognizable, although a sequence of volcaniclastic products covers the deposit. The Arroyo Grande unit is composed of both matrix and

block facies, is massive, poorly sorted, and well consolidated. The matrix is gray-pinkish sand, and the clasts are essentially monolithologic, angular gray dacitic fragments to 1 m in maximum diameter (Fig. 5A). Clasts with jigsaw cracks are common throughout the unit, and some accidental clasts of laminated silty sediments crop out near the base of the deposit. The stratigraphic position of the Arroyo Grande unit was observed in some sections (Fig. 6A). At the base of the unit, a paleosol layer yielded a radiocarbon (^{14}C) date of 40,985 +1370/–1170 yr B.P. This unit underlies a block-and-ash pyroclastic flow deposit ^{14}C dated as ca.13 ka (Macías et al., 1997; García-Palomo et al., 2002). Clast lithologies have a distinct affinity with the El Fraile dome in the crater area (Casartelli, 2004), indicating that the debris avalanche was generated by an east-southeastward sector collapse of a dome in the crater area, probably the El Fraile dome (Fig. 3), between ca. 40 and 13 ka.

The El Zaguán lithostratigraphic unit was first reported by Macías et al. (1997). New observations revealed that is extensively exposed on the eastern flank of the volcano, along several ravines, including the El Zaguán and Cienaga gullies (Fig. 4). This deposit has a maximum thickness of ~30 m and an estimated volume of 0.4 km^3. Hummocky morphology is still clearly recognizable even though the deposit is partly covered by volcaniclastic deposits. The El Zaguán unit comprises at least three discrete flow units of different colors, textures, and degrees of alteration (Fig. 5C). The boundaries between individual flow units are usually deformed where the lower unit intrudes the upper one. It is composed of both matrix and block facies, and is massive, unsorted, and unconsolidated. The clasts are angular to subangular gray-pinkish dacitic fragments to 3 m in maximum diameter, embedded in an ochre-gray-pinkish sandy matrix. Clasts with jigsaw cracks are common throughout the unit. Some accidental clasts, to 1–2 m in maximum diameter, consist of laminated silty lacustrine sediments squeezed and compacted due the load of the overhanging deposit. The stratigraphic position of the El Zaguán unit was observed in some sections (Fig. 6B), but no datable paleosol horizon was found. This unit overlies the 37 ka block-and-ash pyroclastic flow deposit, and is directly overlain by the 28 ka pyroclastic block-and-ash deposit that is discontinuously exposed along the Cienaga gully (Macías et al., 1997; García-Palomo et al., 2002; Caballero and Capra, 2004). In these outcrops, the 28 ka block-and-ash pyroclastic flow deposit is 10 m thick, laminated, with abundant matrix, and with dilutes pyroclastic gravity currents of the surge type. This entire sequence is capped by the 21.7 ka Lower Toluca Pumice plinian fall deposit (Capra et al., 2006). Petrographic and geochemical analyses by Casartelli (2004) revealed a close similarity between the El Zaguán unit and the Cienaga summit dome (Fig. 3); together with stratigraphic evidence, this indicates that the epiclastic deposit was generated by an eastward sector collapse of the Cienaga dome immediately prior to the emplacement of the 28 ka block-and ash pyroclastic flow deposit. The magmatic activity associated with the extrusion of a new lava dome and the consequent overloading of the whole structure, probably promoted and triggered the sector collapse. Subsequently,

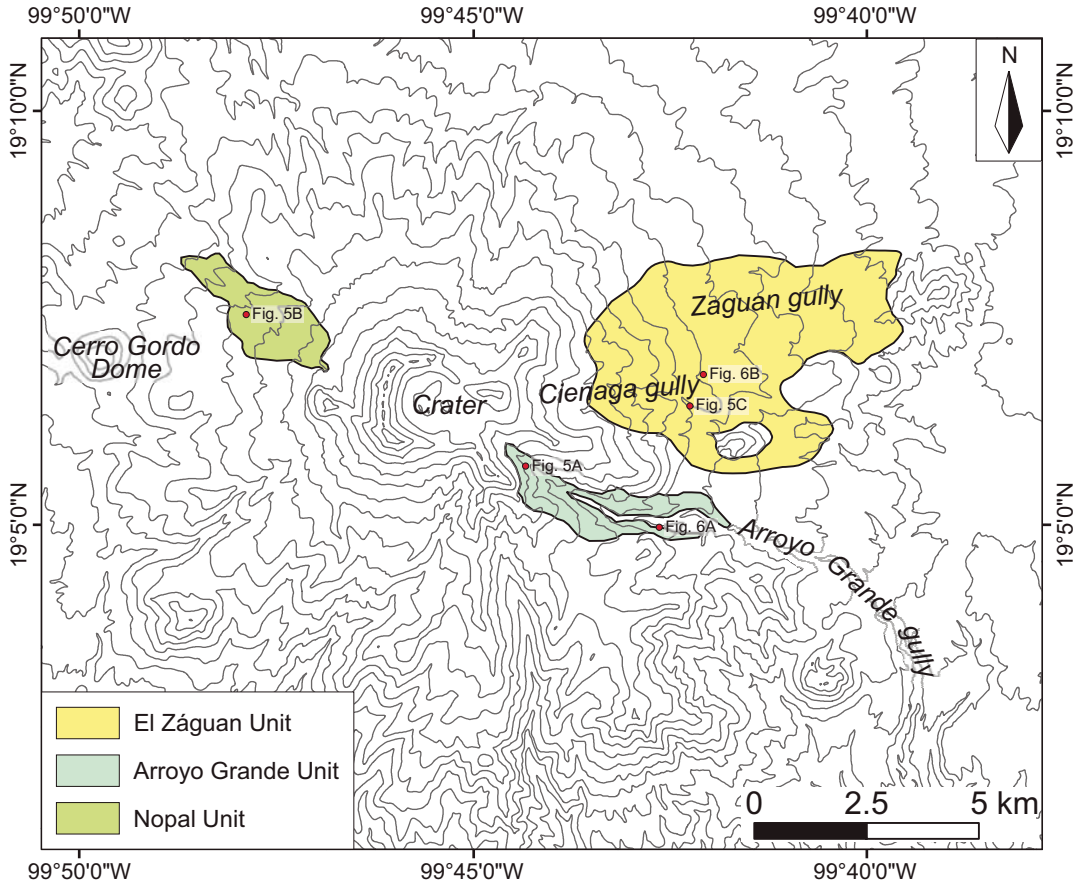

Figure 4. Distribution map of the three debris avalanche deposits younger than 50 ka recognized on Nevado de Toluca Volcano. Locations of pictures and stratigraphic sections represented in Figures 5 and 6 are shown.

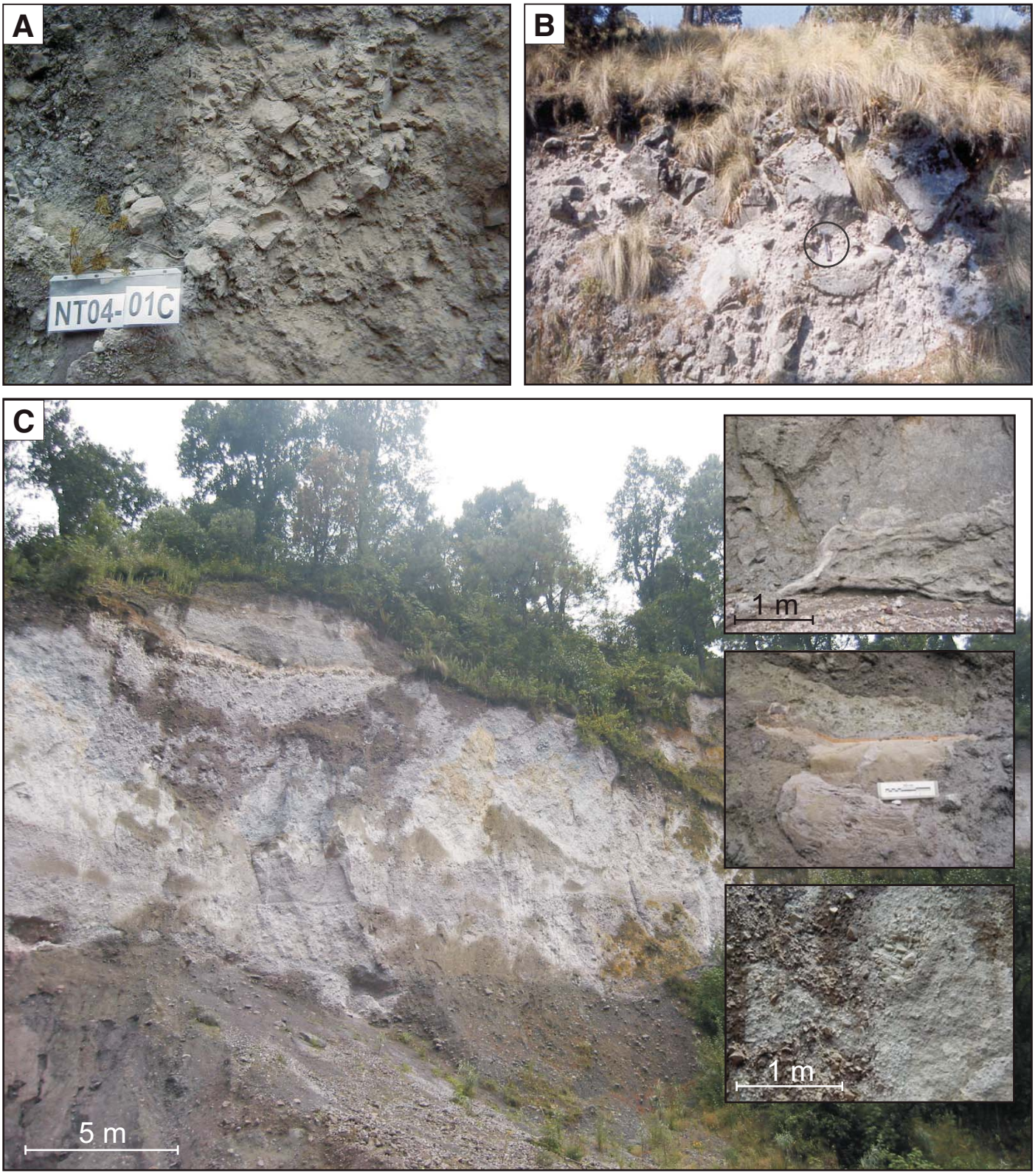

Figure 5. (A) Outcrop of the Arroyo Grande debris avalanche deposit along the Arroyo Grande gully. (B) Outcrop of the Nopal debris avalanche deposit along the unpaved road to the crater, on the northwestern flank of the volcano; hammer in the black circle is 35 cm in length. (C) Outcrops of the Zaguán debris avalanche deposit along the Cienaga gully. Insets are, from top to bottom, clastic dikes at the base of the debris avalanche deposit, fragment of deformed lacustrine sediments imbedded in the deposit, and clasts with jigsaw cracks.

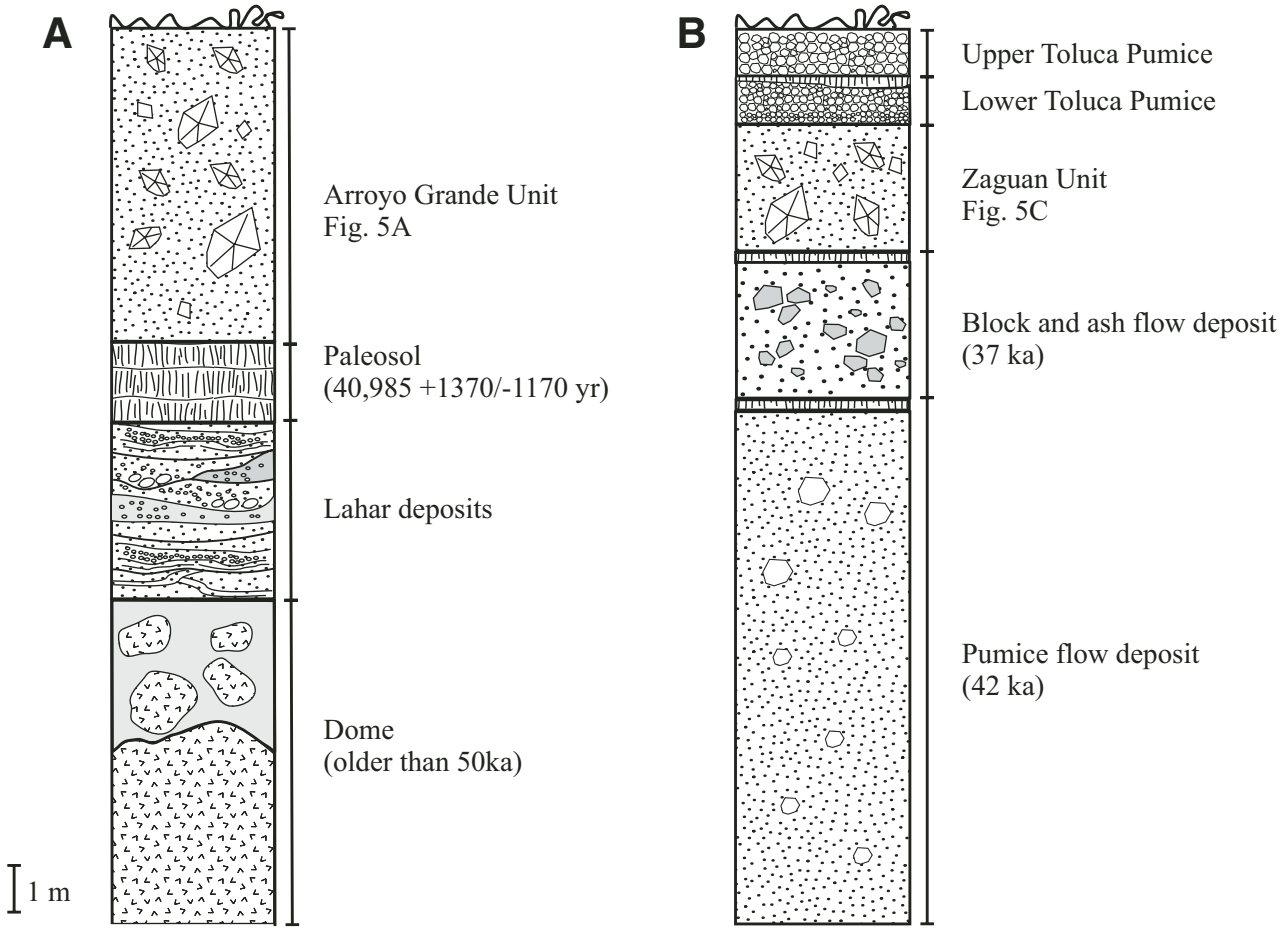

Figure 6. Stratigraphic sections showing stratigraphic position of the Arroyo Grande (A) and Zaguán (B) units.

Merapi-type eruptions generated the main part of the 28 ka block-and-ash flow deposit, with radial distribution on the volcano flanks.

The Nopal lithostratigraphic unit is a debris avalanche deposit that crops out discontinuously within a limited portion of the western flank of the volcano (Fig. 4) with exposed thicknesses ranging between 2 and 15 m. The deposit surface exhibits linear ridges aligned along the 290° azimuth, parallel to the flow direction. The unit is massive, poorly sorted, and well consolidated. It is both matrix and clast supported. Its matrix is variably gray-pinkish and sandy, and its subangular clasts are monolithologic, gray-pinkish dacite to 2 m in maximum diameter (Fig. 5B). Jigsaw cracks are common throughout the deposit. The stratigraphic position of the unit is difficult to define, but geometric relationships suggest that it is above the 28 or 37 ka block-and-ash pyroclastic flow deposit (Macías et al., 1997; García-Palomo et al., 2002). The Nopal unit is covered by the 10.5 ka Upper Toluca Pumice deposit. Petrographic and geochemical analyses (Merlini, 2004) revealed a strong correlation between the Nopal unit and the Nieve summit dome (Fig. 3), indicating that the Nopal debris avalanche was generated by a west-northwestward sector failure of the Nieve dome between 37 and 10.5 ka.

Morphological and Structural Data

During the last eruptive phase of Nevado de Toluca volcano (after 50 ka), the tectonics of the area was dominated by the Tenango fault system, the youngest and most active fault system in the area (Fig. 1B). It consists of main fault planes striking along the 90°–120° azimuths and minor faults and fractures striking at 30°–60° azimuths (García-Palomo et al., 2000; Norini et al., 2006). Norini et al. (2006) suggested an active left-lateral oblique-slip transtension for this system with a ratio of sinistral to normal slip between 3:2 and 5:2, a minimum age of 700–800 ka, and a Holocene slip rate of ~0.3–0.5 mm/yr. Morphostructural analysis has revealed a strong influence of this tectonic activity on Nevado de Toluca volcano (Norini et al., 2004). In shaded relief images, lineaments of the Tenango fault system strike across the edifice approximately along the 110° azimuth, defining a narrow graben-like structure (Fig. 7), reflecting the geometry and style of deformation in the edifice interior (Fig. 2C). Topographic profiles show how the surface expression of this graben is marked by small sharp scarps in the lower flank of the volcano, while on the summit it is almost masked by the recent dome complex, which defines an area of very steep outward sides (Fig. 7). The graben is partially filled by the most recent (younger than 50 ka) pyroclastic and epiclastic deposits of the volcano (Fig. 2B), and these deposits are faulted by the Tenango fault system (Norini et al., 2006). The volcanic activity in the past 50 k.y. and the deformation along the Tenango fault system were contemporary and the close temporal and spatial association between recent volcanism and brittle deformation structures suggests a control of the tectonics on the evolution of Nevado de Toluca. This interplay is manifested by constructional features like the dome complex as well as the distribution of debris avalanche deposits, which are spatially correlated with the active faults in the area (Fig. 8). Although in the

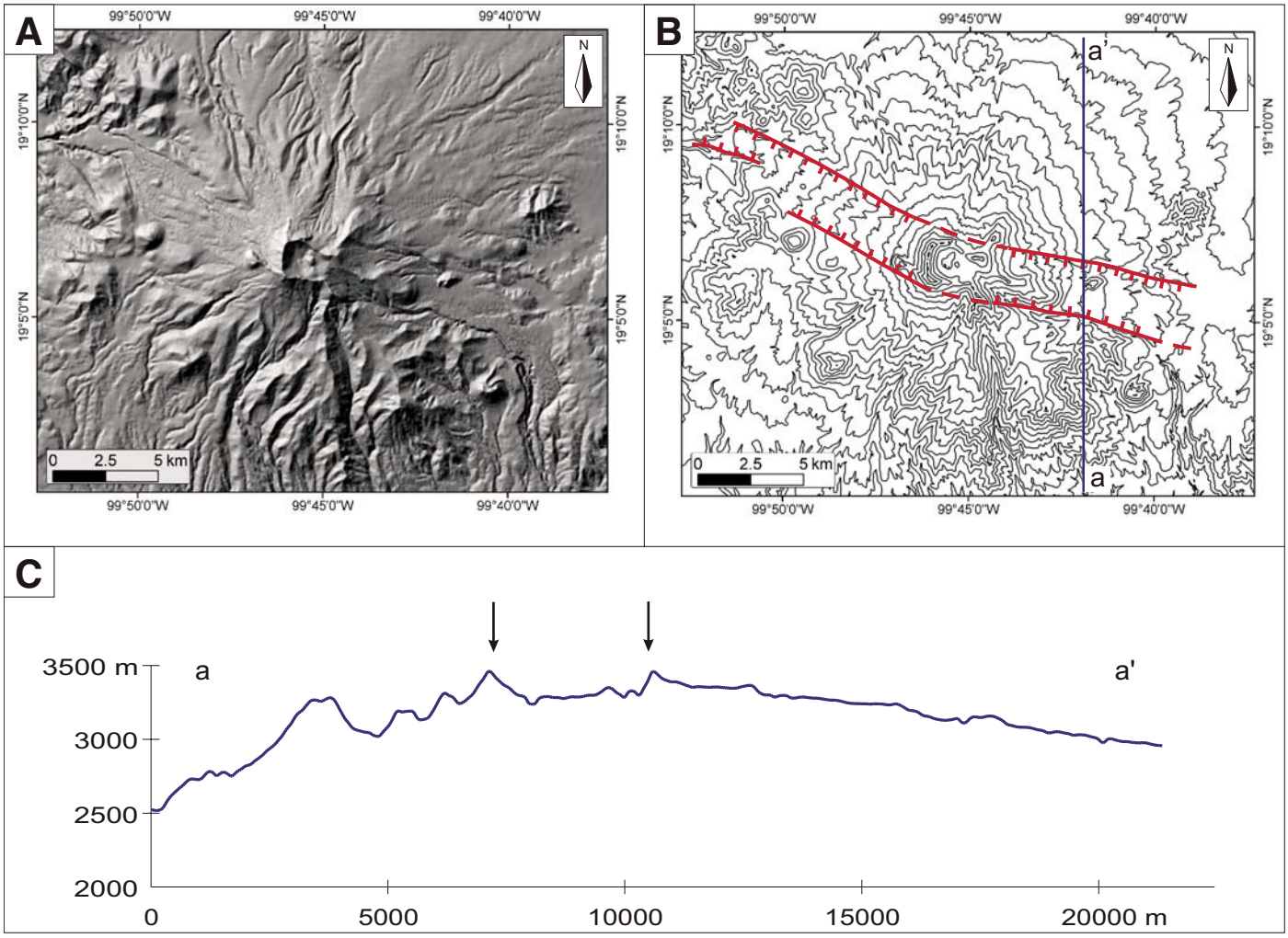

Figure 7. Shaded relief image (A) and contour map (B) of the studied area showing the narrow graben-like structure that strikes east-west and west-northwest–east-southeast across the Nevado de Toluca Volcano. (C) Topographic profile depicts the morphology of the graben in the middle-lower flank of the volcano (black arrows).

summit region of the volcano the topographic gradient of the flanks is similar in all the directions, debris avalanche deposits were emplaced only toward east and west along the Tenango fault system (Figs. 7 and 8). Therefore the distribution of these deposits shows there is a control of the tectonics over the directions of sector collapses. The 13-km-long and 4-km-wide spatial distribution of the dome complex trends parallel to the Tenango fault system (Figs. 2B and 3; Supplemental File 1 [see footnote 1]). This configuration indicates that a feeding system aligned along the Tenango fault system structure acts as a preferential pathway for magma. A detailed morphostructural analysis of the summit also shows the control of basement tectonics on the development of the dome complex. From aerial photographs stereopairs, we drew the morphological boundary related to each summit dome (Fig. 9); then, using an image processing program (ImageJ), we obtained the smallest elliptical envelop of every dome. In the processed image we measured essential parameters of the dome geometry as the azimuths of the major axis of the elliptical envelopes (elongation axis) (Table 1). The rose diagrams showing the length and orientation of the elongation axis of the domes depict two main structural trends: azimuths ~85° and ~120° (Fig. 10). Other identifiable lineament trends are oriented roughly along azimuths 5° and 40° (Fig. 10). Geological data support identification of age relationships among these different structural trends. In Nevado de Toluca volcano, domes with a major axis oriented at azimuth ~5° and ~40° are younger than domes oriented along azimuths ~85° and ~120° (Figs. 3 and 9; Table 1). Thus, the structural evolution of the crater area in the past 50 k.y. underwent a sharp change in the orientation of the feeding system from about east-west to north-south in response to Tenango fault system tectonics. This fault system influenced the crater morphology of the summit of Nevado de Toluca, creating an offset in the southwestern rim of the present crater and forming a ridge at the western flank of the volcano's summit (Norini et al., 2006) (Fig. 11).

ANALOGUE MODELING OF VOLCANO-BASEMENT INTERACTION

To gain insights about the evolution of Nevado de Toluca volcano, the geological and structural data from the field were applied to construct a brittle-analogue model of a cone made of granular material on a sheared basal layer. This model is similar to those of van Wyk de Vries and Merle (1998), Lagmay et al. (2000), Wooller (2004), and Norini and Lagmay (2005). The movement vector is at an angle relative to the

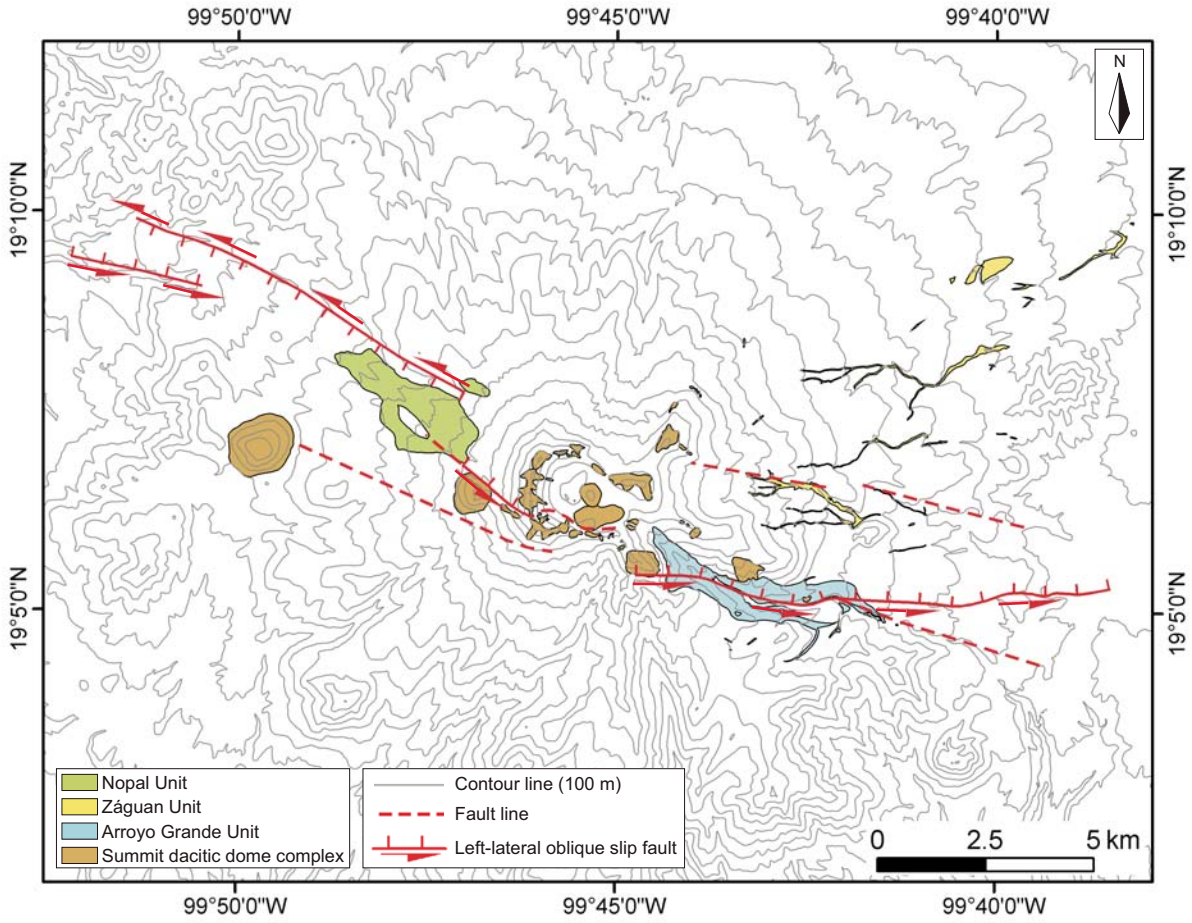

Figure 8. Geological map depicting the volcanic and tectonic activity in the Nevado de Toluca volcano in the past 50 k.y. (see Supplemental File 1 [see footnote 1]). Outcrops of the debris avalanche deposits and dacitic dome complex are shown as well as the main structures of the Tenango fault system.

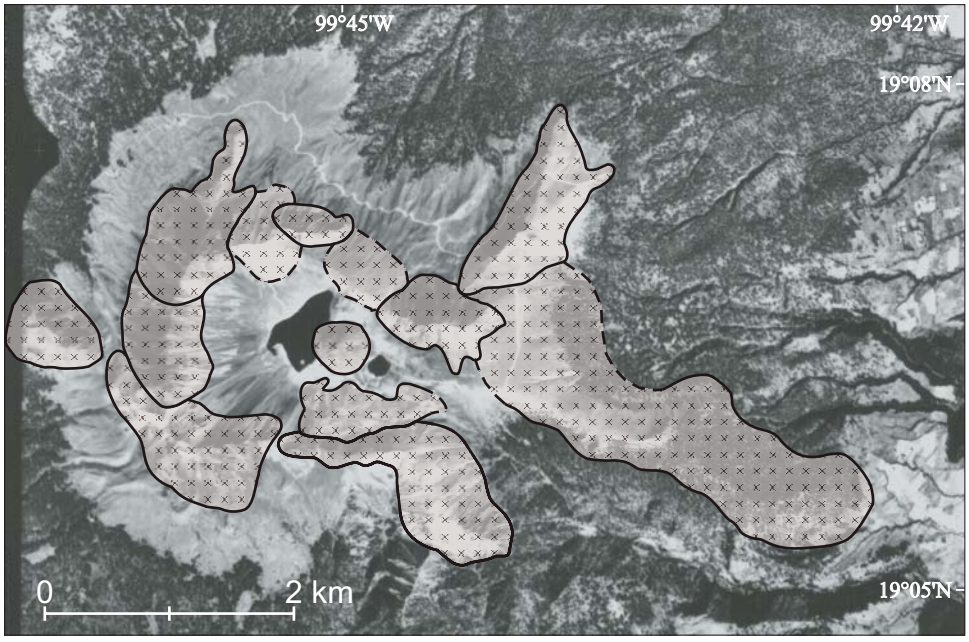

Figure 9. (A) Outline map of the domes recognized in the crater area on a black and white 1:75,000 aerial photograph [Instituto Nacional de Estadística Geografía y Informática (INEGI)]; the boundaries represent the morphological appearance of each dome (see Table 1).

TABLE 1. MORPHOLOGICAL PARAMETERS OF THE DOMES COMPOSING THE SUMMIT DOME COMPLEX

Dome	R_{max}/R_{min}	Azimuth (°)	Maximum length (km)
El Fraile	1.80	126	1.5
Matador	1.95	116	1.9
Cienaga	1.94	117	3.7
Nieve	1.41	129	0.8
Sella	1.36	125	0.7
Corno	1.11	87	0.6
Luna	1.23	91	1.0
Nunca	1.92	95	0.7
Rojo	1.66	4	1.3
Volcan	1.68	19	1.5
Pico	1.87	41	1.5
Cerro	1.81	77	1.2
Ombligo	1.15	92	0.5

Note: R_{max}/R_{min}—ratio between the major and minor axes of the smallest elliptical envelope of the dome outline. Azimuth—orientation of the major axis of the envelope. Maximum length—maximum length of the dome along the major axis of the envelope.

long dimension of the basal plate (Fig. 12), and a transtensive left-lateral motion is generated, mimicking that of the Tenango fault system that deforms Nevado de Toluca, as suggested by Norini et al. (2006). The experimental apparatus consists of a basal plate attached to a vertical side plate that in turn is fastened to a screw jack. Rotation of the screw, controlled by computer, induces movement of the basal plate. A ratio of sinistral to normal slip measured in the field was between 3:2 and 5:2 (Norini et al., 2006), and so the length of the basal plate was positioned at a 25° angle relative to the movement vector, simulating an ~2:1 ratio between transcurrent movement and extension normal to the fault. Both the cone and substrate were made of stratified layers, alternately dyed in contrasting colors, consisting of the identical mixture of two sizes (0–70 and 70–200 μm) of dry quartzose granular sand. This mixture has an angle of internal friction (Φ) of ~30° and cohesion (*C*) of ~25 Pa. Resting on the base plate, the substrate for the cone was simulated with a 3.5-cm-thick layer of the mixture with plan dimensions of 50 × 40 cm. The experiments were photographed to record the structures that developed during progressive transtensive movement. Completed experiments were wetted and then sliced parallel and perpendicular to the fault strike, to reveal the structures within the cone in three dimensions as seen in deformations of the colored layers.

Model Scaling

Model parameters have to be geometrically, kinematically, and dynamically scaled in order to ensure similarities between natural prototype and experimental results (Hubbert, 1937; Ramberg, 1981; Galland et al., 2006). The main forces to consider for correct scaling are body forces due to gravity and stresses. The dimensionless ratio between body forces and stresses can be defined:

$$\Pi = \frac{\rho \times g \times l}{\sigma}, \quad (1)$$

where ρ is the rock density, *g* is the gravity, *l* is the linear dimension, and σ is the tectonic stress. The ratio Π must be similar in nature and in the model for the scaling of the analogue

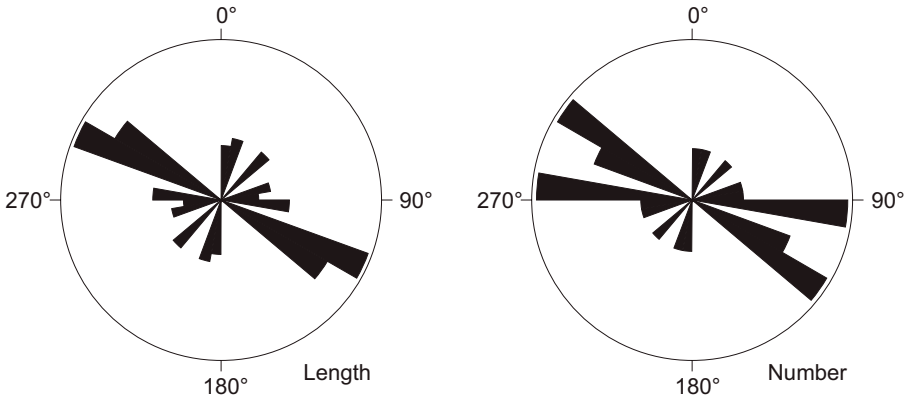

Figure 10. Rose diagrams showing azimuth of the major axis of the smallest elliptical envelope of the domes forming the summit dome complex (Table 1). The azimuths are plotted based on length and number of domes.

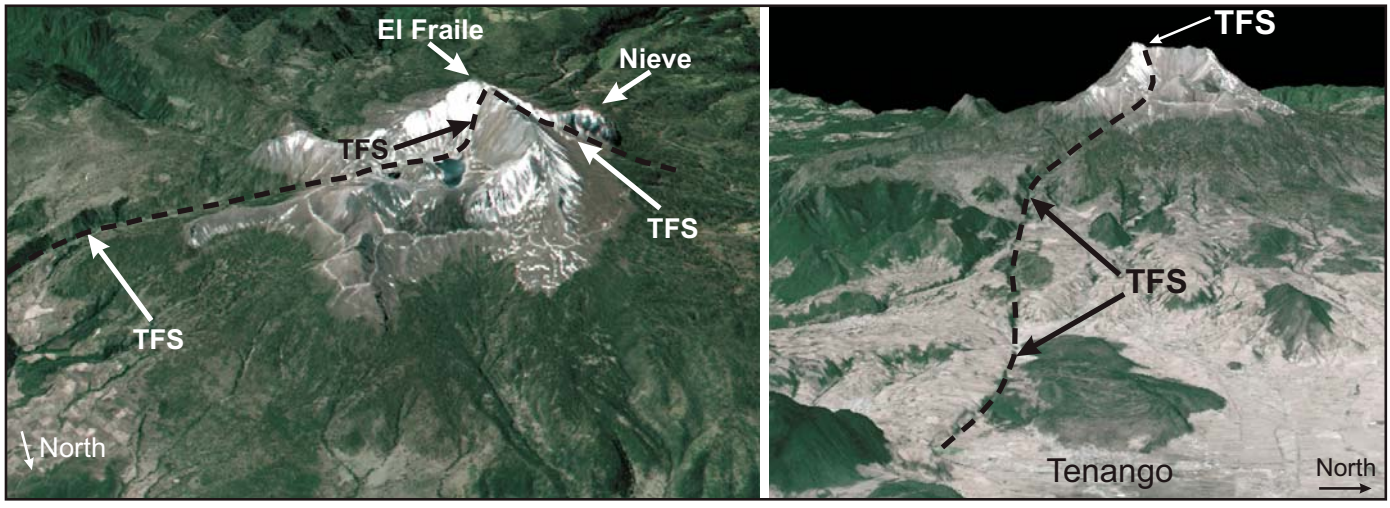

Figure 11. Effects of Tenango fault system (TFS) faulting on the crater of Nevado de Toluca revealed by perspective views from north and east of the volcano; both views were generated from digital elevation model and Aster satellite images. Arrows indicate the TFS trace and offset in the southwestern rim of the present crater.

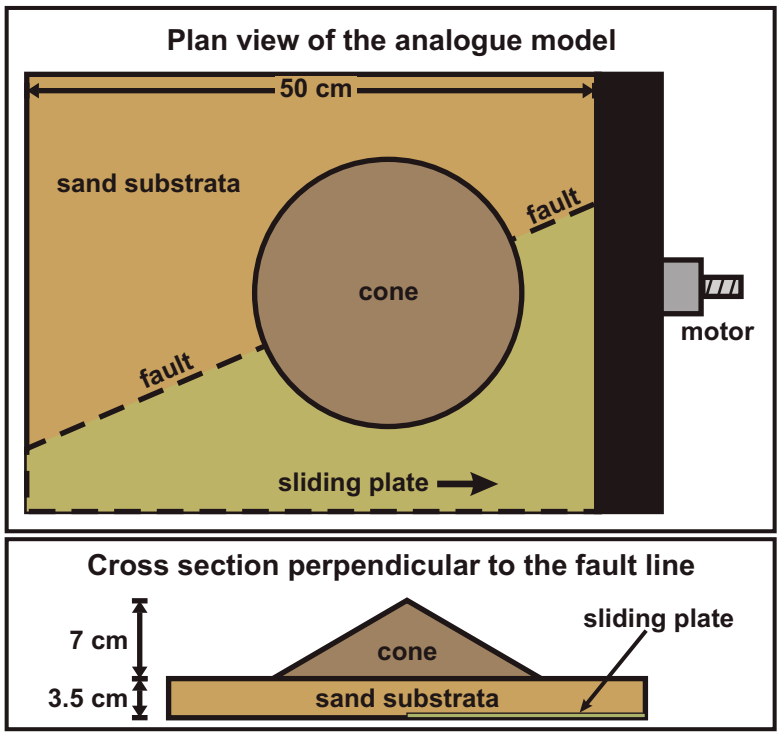

Figure 12. Schematic plan view and cross section of the analogue model, showing the substrate layer of sand and cone that represent the volcanic edifice. The layer of sand partly rests on top of a sliding plate, which is attached to a side plate. The side plate is pulled by a screw jack, which moves according to a desired rate specified by a computer. Oblique-slip shearing is generated along the tilted margin of the basal plate when the screw jack is pulled.

experiment to be correct. Therefore, the stress ratio (σ^*) between model and nature can be calculated from:

$$\sigma^* \approx \rho^* \times g^* \times l^*, \quad (2)$$

where ρ^* is the density ratio, g^* is the gravity ratio, and l^* is the length ratio between model and nature. The experiments were conducted in the Earth's field of gravity; consequently the model/nature ratio for the gravitational acceleration (g^*) was unity. The length ratio, which is on the order of 10^{-5}–10^{-4}, varies with the model dimension and can be used to fit the required stress ratio considering the density of the analogue material. The Nevado de Toluca summit is 4680 m above sea level, the surrounding Lerma basin is at 2600 m elevation, and therefore the height of the volcanic cone is ~2000 m. The experimental cone was 7–8 cm high and the resulting length ratio (l^*) was 4×10^{-5} (geometric scale 1:25,000). The rocks in a composite volcano like Nevado de Toluca include high-density mafic lavas and very low density pyroclastic deposits (Bellotti et al., 2004), and so the mean density is difficult to estimate. An andesitic-dacitic stratovolcano reasonably similar in dimension, composition, and eruptive style is Mount St. Helens (Lipman and Mullineaux, 1981), for which a mean density of 2.15 g/cm^3 was calculated using geophysical methods (Williams et al., 1987). The sand used in the analogue experiments has a density of 1.4 g/cm^3 and so the density ratio (ρ^*) was 0.65. Therefore, the dimensionless stress ratio (σ^*) between the brittle analogue model and Nevado de Toluca volcano was $\sim 2.6 \times 10^{-5}$, meaning that the model was ~38,000 times weaker than its natural counterpart. For the rocks of the volcanic edifice, we assume a linear Mohr-Coulomb failure criterion, where the parameters are the cohesion C and the angle of internal friction Φ (Byerlee, 1978). For competent volcanic rocks the cohesion is in the order of 10^7–10^8 Pa and the angle of internal friction is ~30°–35°, but for incompetent rocks the cohesion can be more than two orders of magnitude smaller (Schellart, 2000). Nevado de Toluca is primarily an altered and a faulted and fractured stratovolcano composed of alternating lava and unconsolidated volcaniclastic deposits (Capra and Macías, 2000; Bellotti et al., 2004), and so the cohesion we assumed was 10^6 Pa. As the cohesion has the dimension of stress, the ratio for cohesion C^* is in the same range as σ^*. In our experiments C^* must be scaled at $\sim 2.6 \times 10^{-5}$ to be equal to the stress ratio σ^*. This requires the use of a material with $C \approx 26$ Pa, which fits the properties of the granular material we used to simulate the volcanic edifice ($C \approx 25$ Pa, $\Phi \approx 30°$). The fault velocity in the experiments was 1 cm/h and the total amount of displacement was 2 cm. Considering the geometric scale of the analogue model (1:25,000), the equivalent fault displacement in nature was 500 m. In agreement with the structural data on the kinematics of the Nevado de Toluca basement, this value has a magnitude similar to that of the total displacement estimate along the Tenango fault system (Norini et al., 2006). The mean slope of Nevado de Toluca is ~10°–15°, but we do not choose to reproduce exactly the geometry of the volcano, but rather to build the analogue cones at the ~30° maximum angle of repose in order to introduce an incipient instability. As demonstrated previously (Norini and Lagmay, 2005), this was necessary because the very low mass of the collapsing sector in analogue models implies that the correct scaling is valid for the structural analysis, but it became less accurate in the analysis of the collapse event. Also, in the analogue models effects such as pore pressure and grain-size reduction along fault zones cannot be taken into account. Considering the balance of forces in the sand models, the mass of the analogue cone is much too small for gravitational pull to induce enough acceleration to simulate the flow of debris avalanches. Furthermore, the steep flanks and the consequent higher mass of the cone slightly improve the scaling of the model, yielding a better reproduction of the effect of volcanic edifice load both on the volcano and on the basement.

Modeling Results

We conducted 10 experiments in which a cone was subjected to basal left-lateral transtension. Boundary conditions, materials, and displacement rates were the same in all the experiments, and the results invariably show the same structures in terms of geometry and kinematics. Thus, the analogue modeling is repeatable. In the experiments, after 3–4 mm of basal plate movement, fractures and faults developed in the cone and basement above the underlying shear, seen both in plan views and cross sections. The deformation in each experimental analogue cone and its substrate was confined to a narrow graben on its surface, bounded by faults parallel to the basal shear (Fig. 13; Animation 1). In the basement, two sets of faults and minor frac-

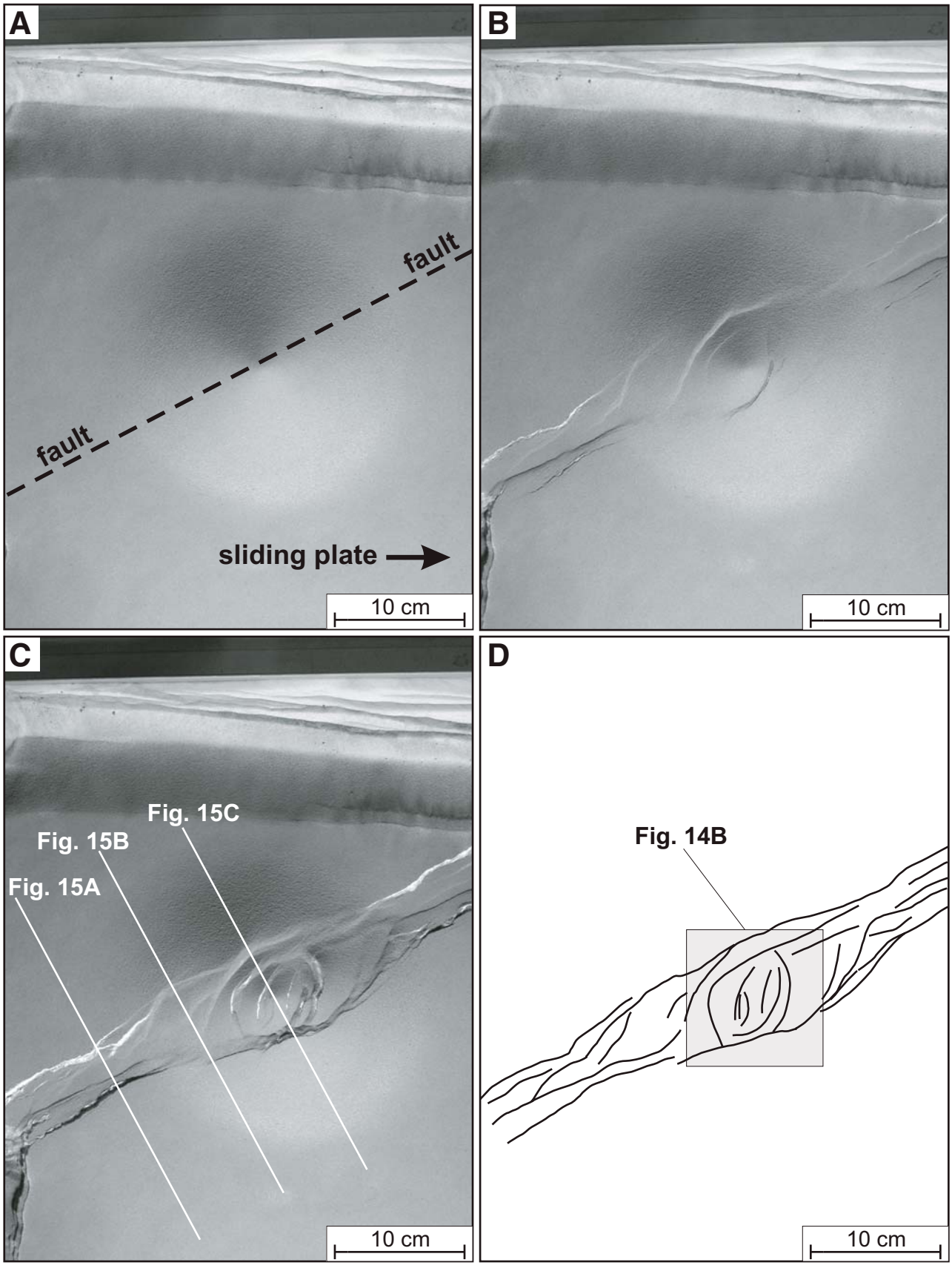

Figure 13. Stages of surface deformation of an analogue cone that is sheared at its base by a left-lateral oblique-slip fault. (A) The cone without deformation. (B) The cone after 0.8 cm of deformation. (C) The cone after 2 cm of deformation. (D) Schematic structural map of the experiment after 2 cm of displacement.

tures developed inside the graben, one oriented parallel to the basal shear, the other ~20°–40° from the main oblique-slip fault line direction. The structures at an angle relative to the basal shear are interpreted as R shears and T fractures, structural terms given to faults characteristic of, but not limited to, strike-slip faulting (Wilcox et al., 1973). As the cone was progressively deformed, the graben consistently bounded unstable areas, which were characterized by a complex set of evolving faults and fractures. At ~1 cm of basal displacement some curvilinear faults and fractures at an angle of ~30° with respect to the main graben boundary developed on the upper flanks of the cone and caused its summit to subside. Between 1 and 2 cm of basal faulting, these curvilinear faults rotated counterclockwise to become perpendicular to the main shear. All the structures on the cone flanks and summit ended sharply at the graben boundary (Fig. 13; Animation 1). Cone instability was promoted by the normal high-angle faults perpendicular to the basal shear confined to the graben and directed toward the cone periphery; thus, sector collapses of the analogue cone were subparallel to the main shear. Orientations of fault and fracture sets developed on the analogue cone were analyzed using rose diagrams. The pictures and data of the models were rotated to make the simulated basal shear parallel to the Tenango fault system; thus, the comparison between the natural prototype and the experiments is easier. At the model scale, the main azimuth direction of faults and fractures is ~115° and subparallel to the basal shear (Fig. 14A). In the summit area of the model cone, several structural trends became apparent. Rose diagrams depict four fracture trends at the summit of the cone, with azimuth directions of 15°, 45°, 80°, and 115° (Fig. 14B). The azimuth 80° and azimuth 115° fractures closely follow the first deformation step and are formed only after 3–4 mm of basal shear. The 15° and 45° trends were last to form and developed after 1 cm of displacement (Fig. 13; Animation 1). In terms of internal structure, the basement outside the cone periphery exhibits high-angle faults that displace marker levels. These structures form a narrow graben (Fig. 15A). Similar faults affect the basement beneath the cone flanks and throughout the cone up to the surface (Fig. 15B). Beneath the cone summit, several subvertical faults displace marker levels in the cone interior and basement, causing the upper part of the cone to subside (Fig. 15C).

COMPARISON BETWEEN NEVADO DE TOLUCA VOLCANO AND THE ANALOGUE MODELS

Three main features that characterize the Nevado de Toluca volcano can be found in the scaled analogue experiments: similar orientations of fracture sets that serve as magma feeding paths during dome emplacement; age relationships of fracture sets developed at the edifice; and type of brittle deformation structures within the edifice. The Nevado de Toluca crater area is composed of elongated domes, preferentially elongated at 5°, 40°, 85°, and 120° azimuths, suggesting that the magma feeding systems are similarly oriented (Fig. 10). Likewise, fracture sets in the analogue experiments are invariably developed at surface orientations of 15°, 45°, 80°, and 115° azimuths (Fig. 14B). Such fracture sets in the cone interior may act as conduits that guide magma toward the surface. The Nevado de Toluca domes elongated parallel to 85° and 120° azimuths are older than domes with 5° elongation. Similarly, in the analogue

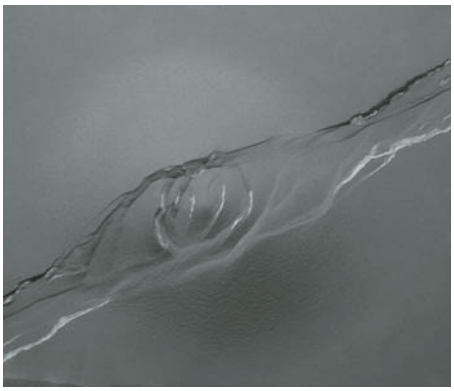

Animation 1. Surface deformation of an analogue cone that is sheared at its base by a left-lateral oblique-slip fault. The video is in compressed AVI format and can be viewed using most free and open-source video player software, such as VLC media player (http://www.videolan.org/vlc). If you are viewing the PDF of this paper or reading it offline, please visit http://dx.doi.org/10.1130/GES00165.SA1 (Animation 1) or the full-text article on www.gsajournals.org to view Animation 1.

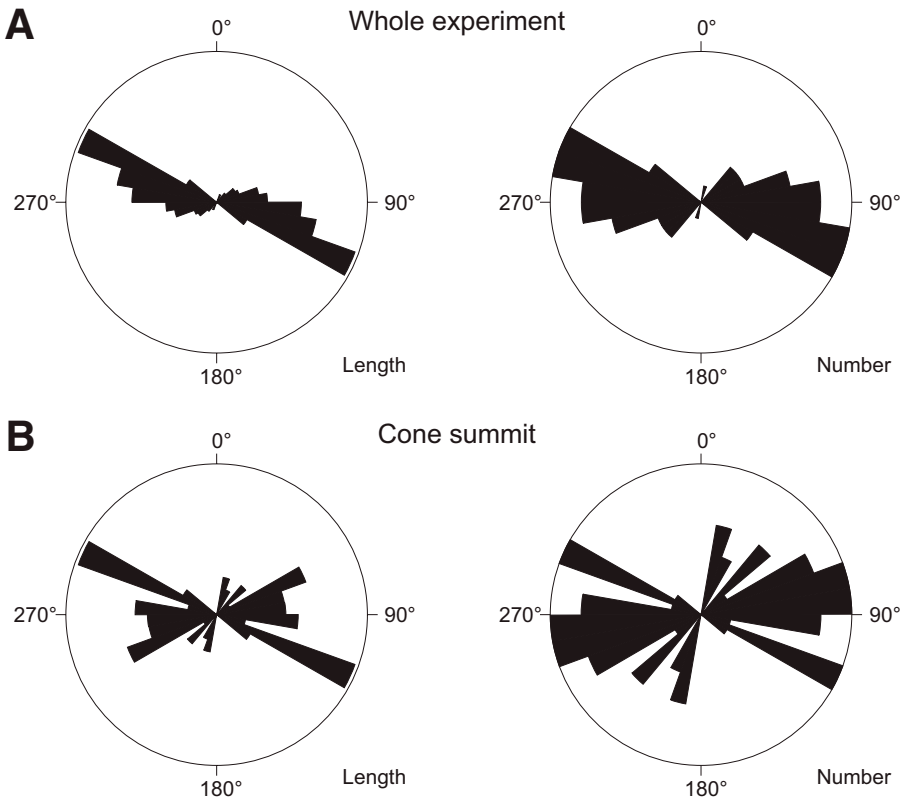

Figure 14. Rose diagrams showing direction of the structures formed at the experiment surface in consequence of left-lateral oblique-slip displacement. The directions are plotted based on length and number of lineaments for the whole experiment (A) and for the summit of the analogue cone (B). The rose diagrams were rotated to make the simulated basal shear parallel to the Tenango fault system.

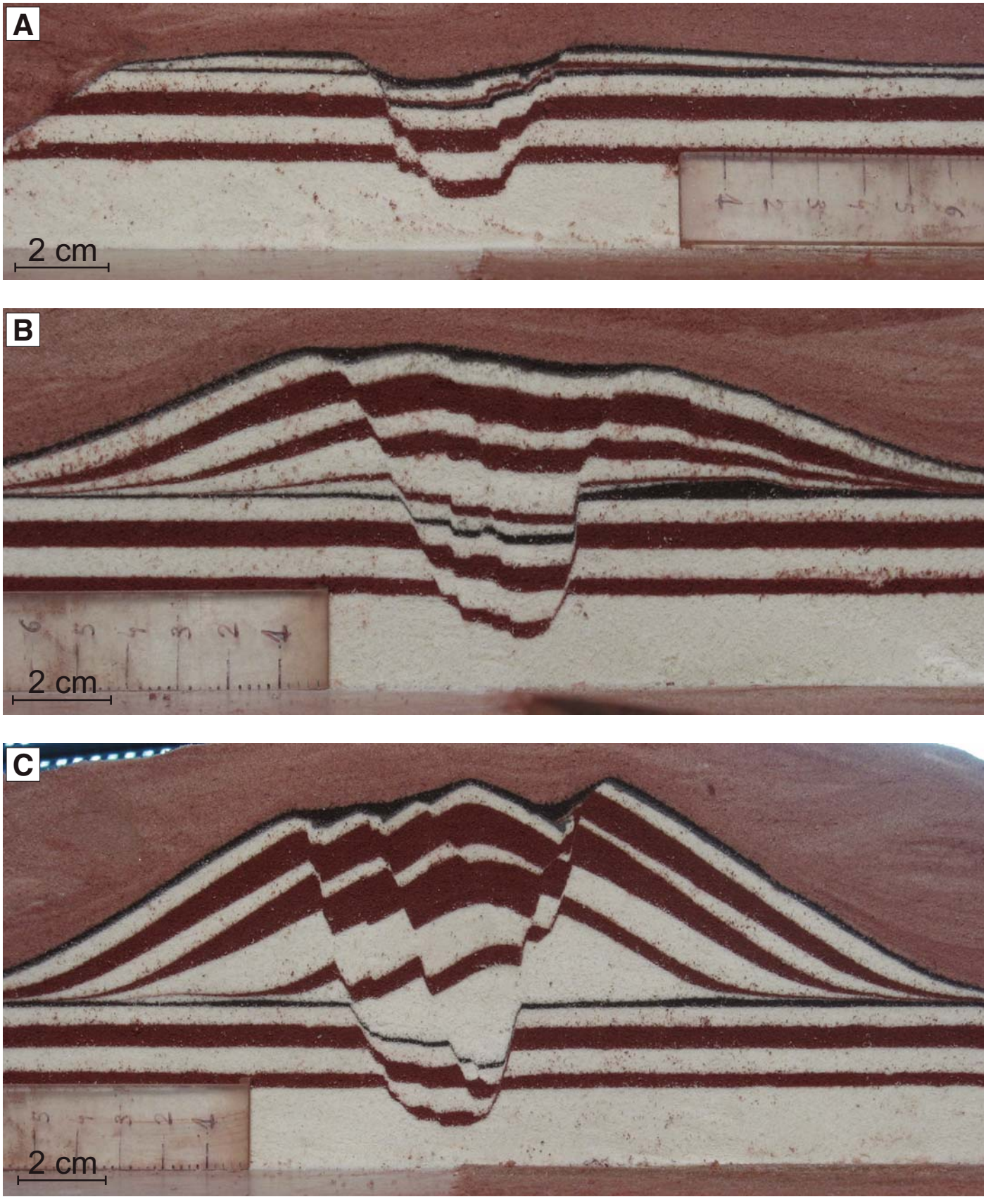

Figure 15. Vertical cross sections of a deformed analogue cone cut perpendicular to the basal shear. Cross sections progress from cuts on the basement (A) toward the summit of the cone (C).

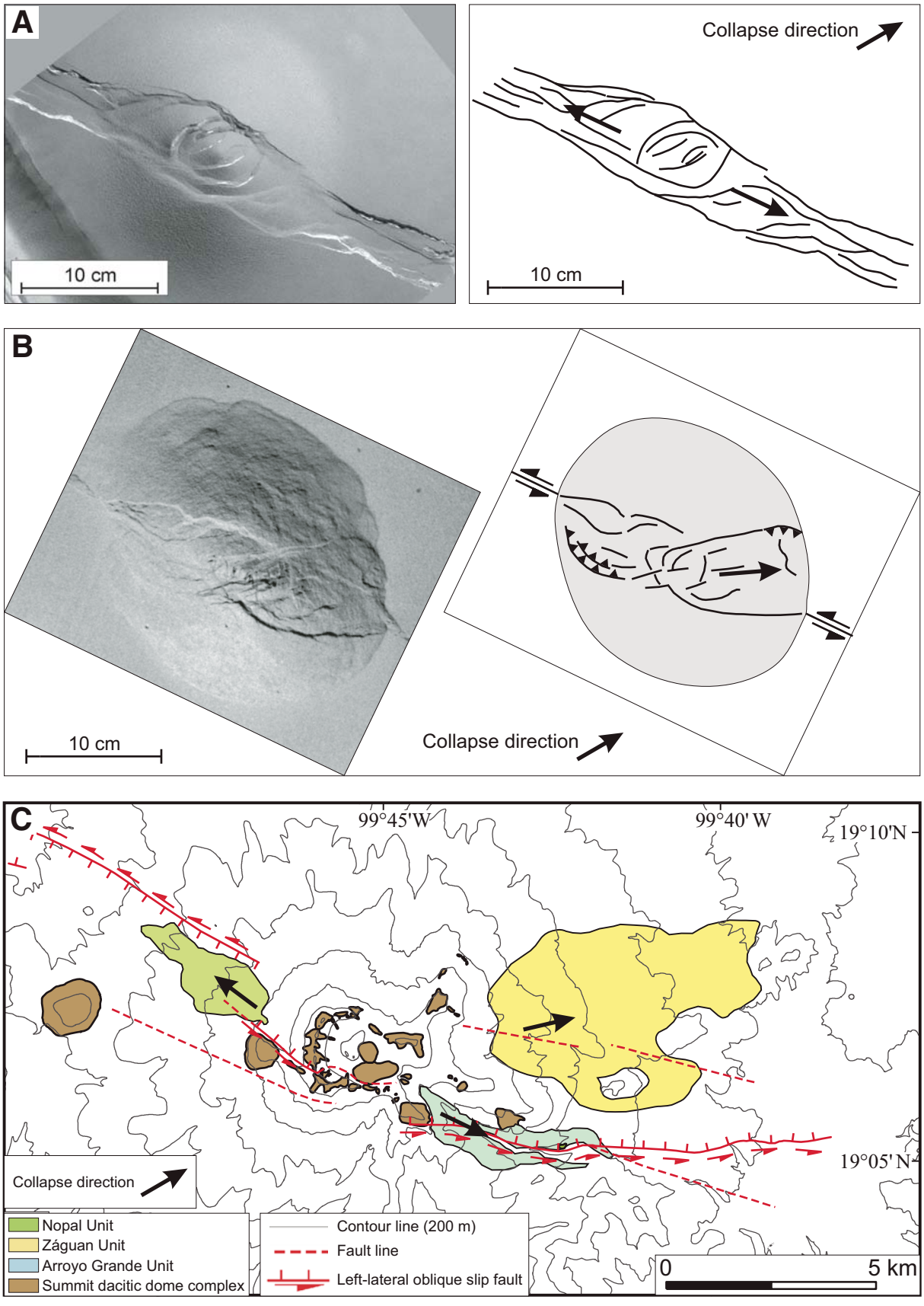

Figure 16. Comparison among instabilities developed on analogue experiments of (A) left-lateral oblique-slip faulting, (B) left-lateral strike-slip faulting (Norini and Lagmay, 2005), and (C) the Nevado de Toluca Volcano in the past 50 k.y.

experiments, faults and fractures that strike 85° and 115° develop earlier than faults and fractures with 15° and 45° strikes. Sections across the deformed analogue experiments display brittle deformation similar to that of the volcano as reconstructed from field and morphostructural data. In both the model and nature, the main structure is a narrow graben that deeply dissects the cone and bounds the sector where magma migrates toward the surface and structural instability can occur (Figs. 2C and 15). In the case of transtension, the collapse directions are nearly parallel to the basement structure (Fig. 16A). Previous analogue modeling of pure transcurrent movements demonstrated that progressive basal displacement leads to collapsing sectors on the cone, with a bisector at an oblique angle of ~30° relative to the underlying strike-slip fault (Lagmay et al., 2000; Norini and Lagmay, 2005) (Fig. 16B). The three documented sector collapses of summit domes occurring on Nevado de Toluca after 50 ka were directed toward the east-southeast, east, and west-northwest, two parallel to the Tenango fault system, the other ~30°–40° from it (Fig. 16C). The sector collapses directed toward the east-southeast and west-northwest were promoted by structures developed on the volcano summit, and the flow of the debris avalanches may have been limited by the sides of the graben. In the case of the El Zaguán debris avalanche deposit, oriented 30°–40° from the Tenango fault system, the collapse direction was mainly controlled by transcurrence-related structures, and the topographic control of gullies may have not been a dominant factor in the general distribution of this deposit (Fig. 16C; Supplemental File 1 [see footnote 1]). Thus, it appears that transtension tectonics played a significant role in the evolution of Nevado de Toluca during the past 50 k.y., especially with respect to dome emplacement and sector collapses. The tectonic control on dome growth and faulting also accounts for crater morphology. Fractures and faults that developed on the summit of the analogue cone generated a square-shaped structure (Fig. 13D), resembling the actual shape of the Nevado de Toluca crater (Figs. 7 and 11). The outline of the crater may be related to the cone load that focuses the initial development of extensional structures, which later evolve toward a transtensional pull-apart basin.

DISCUSSION

The last stage of activity of Nevado de Toluca volcano started ca. 50 ka. During that time, a dome complex formed at the volcano summit and a sequence of volcaniclastic deposits on its flanks was emplaced, including three debris avalanche deposits originating from sector collapses of summit domes. Geological and structural data and analogue modeling clearly show that the edifice was shaped by interaction between the volcanic and tectonic processes, especially activity of the Tenango fault system. Tectonics generated pervasive structures in the cone interior, which may control the rise of magma and consequent eruptions. As a result, the spatial distribution of effusive products younger than 50 ka is confined along the intersections between the Tenango fault system structures and topographic surface (Figs. 2 and 3; Supplemental File 1 [see footnote 1]). The timing of the growth of the dome complex follows the propagation of the Tenango fault system structures inside the volcanic edifice. Magma ascent to the surface is made possible through older transtensive faults subparallel to the Tenango fault system basement fault zone, with azimuth of ~85° and 120°, and younger secondary, mainly normal faults, with azimuths of ~5° and 40°. As revealed by analogue modeling, the mainly normal faults are commonly found directly beneath the volcano summit, sharply bounded at high angles by the transtensive ones. The first domes to be emplaced used structures parallel to the Tenango fault system (azimuth 85° and 120°) as the feeding system. Subsequent effusive events generated domes elongated along azimuths 5° and 40° and were probably emplaced along faults that were formed at later stages of continuous activity of the Tenango fault system. The geometry and kinematics of Tenango fault system not only controlled the volcano growth, but also affected the stability of Nevado de Toluca edifice. The normal faults intersecting at high angles on the volcano summit probably promoted sector collapses in the crater, and the graben in the volcanic cone and its basement guided debris avalanches along this west-northwest–oriented structural depression. Resulting magmatic and nonmagmatic sector collapses affected limited portions of the volcano summit, usually single domes, and formed small monolithologic debris avalanches that deposited the Arroyo Grande, El Zaguán, and Nopal units, each with a volume of ~0.3–0.4 km^3. The collapses were triggered by exogenous or endogenous factors, such as magmatic activity in the case of the El Zaguán debris avalanche deposit, and were guided by structures developed in the cone as a consequence of Tenango fault system transtensive kinematics, including T, R, and R' in the sense of Wilcox et al. (1973). These structures produced collapses directed parallel to the Tenango fault system as well as at an angle of ~30° counterclockwise with respect to the basement fault zone (Lagmay et al., 2000; Norini and Lagmay, 2005), as was the case in the collapse of the Cienaga dome that produced the El Zaguán deposit. The topographic gradient of the graben seems to have no major role in the direction of the sector collapses, but only partial control on flow and spatial distribution of the debris avalanche deposits. This is because the morphological expression of the Nevado de Toluca graben is limited to the middle-lower flank of the volcano and not on its summit, where the collapses originated (Fig. 7). Thus, the expected sector collapse directions in case of future gravitational failures are east-southeast, west-northwest, east, and west. Conversely, load-induced stresses from Nevado de Toluca edifice probably add to regional stresses on the Tenango fault system, affecting its geometry, kinematics, and dynamics. The volcano load can generate an anomaly in the regional stress field, slightly increasing the normal component of motion in the Tenango fault system kinematics and focusing deformation in the crater area. This is because the vertical stress is incremented beneath the volcano in response to the load of the ~2000-m-high volcanic pile (van Wyk de Vries and Merle, 1998; Marques and Cobbold, 2002). The model for the growth and collapse of the Nevado de Toluca volcano presented here accounts for the entire volcano structure, as well as for its sector collapses during the past 50 k.y. From a hazard perspective, the numerous examples of composite volcanoes in continental and island volcanic arcs with similar structural-volcanological characteristics of Nevado de Toluca volcano imply that our model may be used to predict not only collapse directions, but also the mechanism of growth and failure of several active and inactive volcanoes. For such volcanoes, hazard monitoring and vigilance must not be limited to periods of activity, because debris avalanches may occur during their periods of quiescence, when threatened populations are not alert.

ACKNOWLEDGMENTS

We thank Kelvin Rodolfo for useful reviews and detailed manuscript editing. Comments from G. Mattioli, Benjamin van Wyk de Vries, Frank Pazzaglia, Pamela Jansma, and Roberto Molina were also appreciated. We acknowledge Fernando Bellotti, Lizeth Caballero, Micaela Casartelli, Marco D'Antonio, Andrea Gigliuto, Riccardo Lunghi, Anna Merlini, and Damiano Sarocchi for their help with field work. We thank José Luis Macías and José Luis Arce for useful discussions, and Erasmo Bardelli, Angelo Ripamonti, and Ambra Mauri for their assistance in the analogue experiments. The sketch of stratigraphic sections was drawn by Micaela Casartelli, Andrea Gigliuto, and Riccardo Lunghi. This work was financed by a Consejo Nacional de Ciencia y Tecnología (CONACYT J37889-T) grant to Lucia Capra. Gianluca Norini was supported by a grant from the Secretaría de Relaciones Exteriores (SRE) of Mexico (2003). The Ministry of Foreign Affairs of Italy and SRE of Mexico provided travel assistance to Gianluca Groppelli and Gianluca Norini. The ^{14}C age was obtained by Austin Long at

the Radiocarbon Laboratory, Gould-Simpson Building, Tucson, Arizona. ImageJ is a public domain Java image processing program (http://rsb.info.nih.gov/ij/).

REFERENCES CITED

Anderson, S.W., and Fink, J.H., 1990, The development and distribution of surface textures at the Mount St Helens dome, *in* Fink, J.H., ed., Lava flows and domes: IAVCEI Proceedings in Volcanology, Volume 2: Berlin, Springer, p. 25–46.

Arce, J.L., Macías, J.L., and Vázquez-Selem, L., 2003, The 10.5 ka Plinian eruption of Nevado de Toluca volcano, Mexico: Stratigraphy and hazard implications: Geological Society of America Bulletin, v. 115, p. 230–248, doi: 10.1130/0016-7606(2003)115<0230:TKPEON>2.0.CO;2.

Arce, J.L., Cervantes, K.E., Macías, J.L., and Mora, J.C., 2005, The 12.1 ka Middle Toluca Pumice: A dacitic Plinian–subplinian eruption of Nevado de Toluca in central Mexico: Journal of Volcanology and Geothermal Research, v. 147, p. 125–143, doi: 10.1016/j.jvolgeores.2005.03.010.

Bahar, I., and Girod, M., 1983, Controle structural du volcanisme Indonesien (Sumatra, Java-Bali): Application et critique de la methode de Nakamura: Bulletin de la Société Géologique de France, v. 7, p. 609–614.

Bellotti, F., Capra, L., Casartelli, M., D'Antonio, M., De Beni, E., Gigliuto, A., Lunghi, R., Merlini, A., Norini, G., and Sarocchi, D., 2004, Geology of Nevado de Toluca volcano (Mexico): International Union of Geological Science, 32nd International Geological Congress, Florence, Italy, Abstract.

Bellotti, F., Capra, L., Groppelli, G., and Norini, G., 2006, Tectonic evolution of the Toluca Basin and its influence on the eruptive history of the Nevado de Toluca Volcano (Mexico): Journal of Volcanology and Geothermal Research, v. 158, p. 21–36.

Bloomfield, K., and Valastro, S., 1974, Late Pleistocene eruptive history of Nevado de Toluca, central México: Geological Society of America Bulletin, v. 85, p. 901–906, doi: 10.1130/0016-7606(1974)85<901:LPEHON>2.0.CO;2.

Bloomfield, K., and Valastro, S., 1977, Late Quaternary tephrachronology of Nevado de Toluca, Central México: Institute of Geological Sciences: Overseas Geology and Mineral Resources, v. 46, p. 1–15.

Borgia, A., Delaney, P.T., and Denlinger, R.P., 2000, Spreading volcanoes: Annual Review of Earth and Planetary Sciences, v. 28, p. 539–570, doi: 10.1146/annurev.earth.28.1.539.

Byerlee, J., 1978, Friction of rocks: Pure and Applied Geophysics, v. 116, p. 615–626, doi: 10.1007/BF00876528.

Caballero, L., and Capra, L., 2004, Textural characteristics of the 28,000 yr. BP debris avalanche deposit of Nevado de Toluca Volcano: International Association of Volcanology and Chemistry of the Earth's Interior, General Assembly, Volcanism and its Impact on Society, Pucon, Chile, Abstract.

Cantagrel, J.M., Robin, C., and Vincent, P., 1981, Les grandes etapes d'evolution d'un volcan andesitique composite: Exemple du Nevado de Toluca: Bulletin of Volcanology, v. 44, p. 177–188, doi: 10.1007/BF02597703.

Capra, L., and Macías, J.L., 2000, Pleistocene cohesive debris flows at Nevado de Toluca Volcano, central Mexico: Journal of Volcanology and Geothermal Research, v. 102, p. 149–168, doi: 10.1016/S0377-0273(00)00186-4.

Capra, L., Macías, J.L., Scott, K.M., Abrams, M., and Garduño-Monroy, V.H., 2002, Debris avalanches and debris flows transformed from collapses in the Trans-Mexican Volcanic Belt, Mexico—Behavior, and implication for hazard assessment: Journal of Volcanology and Geothermal Research, v. 113, p. 81–110, doi: 10.1016/S0377-0273(01)00252-9.

Capra, L., Carreras, L., Arce, J.L., and Macías, J.L., 2006, The lower Toluca pumice: A ~21,700 yr B.P. Plinian eruption of Nevado de Toluca volcano, México, *in* Siebe, C., et al., eds., Neogene-Quaternary continental margin volcanism: A perspective from México: Geological Society of America Special Paper 402, p. 155–173.

Casartelli, M., 2004, Evoluzione geologica del Nevado de Toluca (Messico): studio stratigrafico, petrografico e geochimico del versante orientale [Tesi di Laurea]: Milano, Università degli Studi di Milano, 231 p.

Day, S.J., 1996, Hydrothermal pore fluid pressure and the stability of porous, permeable volcanoes, *in* McGuire, W.J., et al., eds., Volcano instability on the Earth and other planets: Geological Society of London Special Publication 110, p. 77–93.

Donnadieu, F., and Merle, O., 1998, Experiments on the indentation process during cryptodome intrusions: New insights into Mount St. Helens deformation: Geology, v. 26, p. 79–82, doi: 10.1130/0091-7613(1998)026<0079:EOTIPD>2.3.CO;2.

Elsworth, D., and Voight, B., 1996, Evaluation of volcano flank instability triggered by dike intrusion, *in* McGuire, W.J., et al., eds., Volcano instability on the Earth and other planets: Geological Society of London Special Publication 110, p. 45–53.

Ferrari, L., 2000, Avances en el conocimiento de la Faja Volcánica Transmexicana durante la última década: Boletin de la Sociedad Geologica Mexicana, v. 53, p. 84–92.

Fink, J.H., and Pollard, D.D., 1983, Structural evidence for dikes beneath silicic domes, Medicine Lake Highland Volcano, California: Geology, v. 11, p. 458–461, doi: 10.1130/0091-7613(1983)11<458:SEFDBS>2.0.CO;2.

Finn, C.A., Sisson, T., Deszcz-Pan, M., and Anderson, E.D., 2004, Mapping weak, altered zones with aerogeophysical measurements at Mount Rainier and Mount Adams, Washington: Implications for volcanic instability: Pucon, Chile, International Association of Volcanology and Chemistry of the Earth's Interior, General Assembly, Volcanism and Its Impact on Society, Abstract.

Francis, P., and Wells, A., 1988, LANDSAT Thematic Mapper observations of debris avalanche deposits in the Central Andes: Bulletin of Volcanology, v. 50, p. 258–278, doi: 10.1007/BF01047488.

Galland, O., Cobbold P., Hallot, E., and de Bremond d'Ars, J., 2006, Use of vegetable oil and silica powder for scale modelling of magmatic intrusion in a deforming brittle crust: Earth and Planetary Science Letters, v. 243, p. 786–804.

García-Palomo, A., Macías, J.L., and Garduño-Monroy, V.H., 2000, Miocene to Recent structural evolution of the Nevado de Toluca volcano region, central Mexico: Tectonophysics, v. 318, p. 281–302, doi: 10.1016/S0040-1951(99)00316-9.

García-Palomo, A., Macías, J.L., Arce, J.L., Capra, L., Espíndola, J.M., and Garduño-Monroy, V.H., 2002, Geology of Nevado de Toluca Volcano and surrounding areas, central Mexico: Geological Society of America Map and Chart Series MCH099, 14 p.

Hubbert, M.K., 1937, Theory of scale models as applied to the study of geologic structures: Geological Society of America Bulletin, v. 48, p. 1459–1520.

Lagmay, A.M.F., and Valdivia, W., 2006, Regional stress influence on the opening direction of crater amphitheatres in Southeast Asian volcanoes: Journal of Volcanology and Geothermal Research, v. 158, p. 139–150.

Lagmay, A.M.F., van Wyk de Vries, B., Kerle, N., and Pyle, D.M., 2000, Volcano instability induced by strike-slip faulting: Bulletin of Volcanology, v. 62, p. 331–346, doi: 10.1007/s004450000103.

Lipman, P.W., and Mullineaux, D.R., 1981, The 1980 eruptions of Mount St. Helens, Washington: U.S. Geological Survey Professional Paper 1250, 844 p.

Macías, J.L., Arce, J.L., García-Palomo, A., Siebe, C., Espíndola, J.M., Komorowski, J.C., and Scott, K., 1997, Late Pleistocene–Holocene cataclysmic eruptions at Nevado de Toluca and Jocotitlan volcanoes, central Mexico, *in* Link, K.P., and Kowallis, B.J., eds., Proterozoic to recent stratigraphy, tectonics and volcanology, Utah, Nevada, southern Idaho and Central Mexico: Brigham Young University Geology Studies, v. 42-I, p. 493–528.

Marques, F.O., and Cobbold, P., 2002, Topography as a major factor in the development of arcuate thrust belts: Insights from sandbox experiments: Tectonophysics, v. 348, p. 247–268, doi: 10.1016/S0040-1951(02)00077-X.

Merlini, A., 2004, Evoluzione geologica del Nevado de Toluca (Messico). Analisi stratigrafica, petrografica e geochimica del versante occidentale [Tesi di Laurea]: Università degli Studi di Milano, 225 p.

Moriya, I., 1980, Bandaian eruption and landforms associated with it, *in* Collection of articles in memory of retirement of Prof. K. Hishimura: Tokio, Tohoku University, v. 66, p. 214–219.

Murray, J., 1988, The influence of loading by lavas on siting of volcanic eruption vents on Mount Etna: Journal of Volcanology and Geothermal Research, v. 35, p. 121–139, doi: 10.1016/0377-0273(88)90010-8.

Nakamura, K., 1977, Volcanoes as possible indicators of tectonic stress: Journal of Volcanology and Geothermal Research, v. 2, p. 1–16, doi: 10.1016/0377-0273(77)90012-9.

Norini, G., and Lagmay, A.M.F., 2005, Deformed symmetrical volcanoes: Geology, v. 33, p. 605–608, doi: 10.1130/G21565.1.

Norini, G., Groppelli, G., Capra, L., and De Beni, E., 2004, Morphological analysis of Nevado de Toluca volcano (Mexico): New insights into the structure and evolution of an andesitic to dacitic stratovolcano: Geomorphology, v. 62, p. 47–61, doi: 10.1016/j.geomorph.2004.02.010.

Norini, G., Groppelli, G., Lagmay, A.M.F., and Capra, L., 2006, Recent left-oblique slip faulting in the central eastern Trans-Mexican Volcanic Belt: Seismic hazard and geodynamic implications: Tectonics, v. 25, p. 1–21, doi: 10.1029/2005TC001877.

Pasquaré, F.A., and Tibaldi, A., 2003, Do transcurrent faults guide volcano growth? The case of NW Bicol Volcanic Arc, Luzon, Philippines: Terra Nova, v. 15, p. 204–212, doi: 10.1046/j.1365-3121.2003.00484.x.

Ramberg, H., 1981, Gravity, deformation and the Earth's crust: New York, Academic Press, 452 p.

Schellart, W.P., 2000, Shear test results for cohesion and friction coefficients for different materials: scaling implications for their usage in analogue modelling: Tectonophysics, v. 324, p. 1–16, doi: 10.1016/S0040-1951(00)00111-6.

Schilling, S.P., Ramsey, D.W., Messerich, J.A., and Thompson, R.A., 2006, Rebuilding Mount St. Helens: U.S. Geological Survey Scientific Investigations Map 2928, http://pubs.usgs.gov/sim/2006/2928/.

Siebert, L., 1984, Large volcanic debris avalanches: Characteristics of source areas, deposits, and associated eruptions: Journal of Volcanology and Geothermal Research, v. 22, p. 163–197, doi: 10.1016/0377-0273(84)90002-7.

Tibaldi, A., 1995, Morphology of pyroclastic cones and tectonics: Journal of Geophysical Research, v. 100, p. 24,521–24,535, doi: 10.1029/95JB02250.

Ui, T., Yamamoto, H., and Suzuki-Kamata, K., 1986, Characterization of debris avalanche deposits in Japan: Journal of Volcanology and Geothermal Research, v. 29, p. 231–243, doi: 10.1016/0377-0273(86)90046-6.

van Wyk de Vries, B., and Merle, O., 1998, Extension induced by volcano loading in regional strike-slip zones: Geology, v. 26, p. 983–986.

Vidal, N., and Merle, O., 2000, Reactivation of basement faults beneath volcanoes: A new model for flank collapse: Journal of Volcanology and Geothermal Research, v. 99, p. 9–26, doi: 10.1016/S0377-0273(99)00194-8.

Voight, B., and Elsworth, D., 1997, Failure of volcano slopes: Geotechnique, v. 47, p. 1–31.

Wilcox, R.E., Harding, T.P., and Seely, D.R., 1973, Basic wrench tectonics: American Association of Petroleum Geologists Bulletin, v. 57, p. 74–96.

Williams, D.L., Abrams, G., Finn, C., Dzurisin, D., Johnson, D.J., and Denlinger, R., 1987, Evidence from gravity data for an intrusive complex beneath Mount St. Helens: Journal of Geophysical Research, v. 92, p. 10,207–10,222, doi: 10.1029/JB092iB10p10207.

Wooller, L.K., 2004, Volcano-tectonic influences on ground deformation and volcanic slope instability: [Ph.D. thesis]: Milton Keynes, UK, The Open University, 183 p.

MANUSCRIPT RECEIVED 19 NOVEMBER 2007
REVISED MANUSCRIPT RECEIVED 16 JUNE 2008
MANUSCRIPT ACCEPTED 18 JUNE 2008